Functional analysis of *parp3* using *Danio rerio* as a vertebrate animal model

Thesis submitted to the Faculty of Graduate and Postdoctoral Studies in partial fulfillment of the requirements for the Master of Science degree
Ottawa-Carleton Institute of Biology
University of Ottawa

Thèse soumise à la Faculté des Études Supérieures et Postdoctorales
En vue de l'obtention de la Maitrise ès Sciences
L'institut de Biologie d'Ottawa-Carleton
Université d'Ottawa

Table of contents

List of figures

List of abbreviations and acronyms

ADPr: Adenosine diphosphate-ribose

ART: ADP-ribosyltransferase

ARTD: ADP-ribosyltransferase-like Diphtheria toxin

BER: base excision repair

bHLH: basic helix-loop-helix

BRCT: Breast Cancer Suppressor Protein (BRCA1), carboxy-terminal domain

ChIP-chip: chromatin immunoprecipitation on chip

ChIP-qPCR: chromatin immunoprecipitation-quantitative Polymerase Chain reaction

DBD: DNA-binding domain

DDR: DNA damage response

DLX: Distal-less homeobox

DSBs: DNA strand breaks

EED: ESC homolog Embryonic Endoderm development

EGFP: Enhanced Green Fluorescent Protein

ESC: Extra sex comb

EST: expressed sequence tag

EZH2: Enhancer of Zeste homologue 2

FOX: Forkhead box transcription fcator

GO: Gene Ontology

HDAC: histone deacetylase

H3K27me3: histone H3 trimethylated on lysine 27

H3K4me3: histone H3 trimethylated on lysine 4

HMG: high mobility group

hPARP: human Poly(ADP-ribose) polymerase

hpf: hour post-fertilization

IRX: Iroquois homeobox protein

ISH: in situ hybridization

IUBMB: International Union of Biochemistry and Molecular Biology

MO: anti-sense morpholino oligonucleotides

NB: neuroblastoma

NC: neural crest

NCC: neural crest cells

NCBI: National center for biotechnology information

neurod: neurogenic differentiation factor

nkx2.1a: NK2 homeobox 1a

NHEJ: non-homologous end joining

pADPr: poly(ADP-ribose)

PARG: poly(ADP-ribose) glycohydrolase

PARP: poly(ADP-ribose) polymerase

PcG: Polycomb group

PRC: Polycomb repressive complex

shh: sonic hedgehog homologue

SK-N-SH: human neuroblastoma cell line

SOX9: sex determining region-Y box 9

SSB: single strand breaks

SSBR: single strand breaks repair

SUZ12: Suppressor 12 of Zeste

sv2: synaptic vesicle 2

TrxG: Trithorax group

vPARP: vault Poly(ADP-ribose) polymerase

XRCC1: X-ray repair cross-complementing I

γH2AX: phosphorylation of histone H2AX

Abstract

PARP1 and PARP2 are the most extensively studied proteins of the poly(ADP-ribose) polymerase (PARP) family. They share partially overlapping functions. These two proteins are best known for their roles in DNA repair. The DNA damage response is actually the most active area of research involving the PARP proteins given the success of PARP inhibitors for cancer therapy. However, PARPs possess many other functions. PARP3, a very little characterized protein, appears to be somewhat involved in the response to DNA damage by genotoxic agents but its physiological function is unknown. Recent evidence indicated that PARP3 is involved in the epigenetic regulation of transcription. For this reason, our collaborators identified PARP3-bound genes by screening the genomic occupancy of PARP3 and found that PARP3-bound genes associate with developmental transcription factors especially involved in neurogenesis. We used zebrafish, a well established vertebrate model in developmental biology, to study the role of PARP3 in development. By knocking-down Parp3 in zebrafish, we found that the loss of Parp3 function reduces the expression of neural crest "specifier" *sox9a* and of *dlx3b/dlx4b*. It impairs the formation of cranial sensory placodes, inner ears and pectoral fins. It delays pigmentation and severely impedes the development of the median fin fold and tail bud. In parallel, the reduced expression of Parp3 leads to a massive increase in apoptosis. I also knocked-down Parp1 and Parp2 in zebrafish. Results suggest that the function of Parp1 is different from that of Parp3 in zebrafish while the data from Parp2 were inconclusive. Our findings demonstrate that Parp3 is essential during early stages of zebrafish development, possibly by exerting its transcriptional regulatory functions during the specification of the neural plate border and by mediating cell survival during the early stages of development.

Résumé

PARP1 et PARP2 sont les deux protéines les plus étudiées de la famille des poly(ADP-ribose) polymerase (PARP). Ils partagent des fonctions partiellement redondantes. Celles-ci sont surtout connues pour leur importance dans la réparation des dommages à l'ADN. La réponse à ces dommages est d'ailleurs le domaine de recherche le plus actif concernant les protéines PARPs et ce, en raison du succès des inhibiteurs de PARPs pour la thérapie contre le cancer. Cependant, ces protéines possèdent d'autres fonctions importantes. PARP3, qui est très peu caractérisée jusqu'à maintenant, semble être impliquée plus modestement dans la réponse aux dommages à l'ADN par des agents génotoxiques et sa fonction physiologique demeure inconnue. De récentes études ont indiqué que PARP3 serait impliquée dans la régulation épigénétique de la transcription. Pour cette raison, nos collaborateurs ont procédé au criblage des gènes qui se lient à PARP3 et ont révélé que la majorité de ces gènes sont des facteurs de transcription impliqués dans le développement, plus spécifiquement dans la neurogénèse. Nous avons utilisé le poisson-zèbre comme modèle vertébré pour l'étude de la fonction de PARP3 au cours du développement. Grâce au « knock-down » de Parp3 chez le poisson-zèbre nous avons découvert que la perte de Parp3 altère l'expression du spécificateur de la crête neurale, *sox9a*, et des gènes *dlx3b/dlx4b*. La perte de Parp3 altère aussi la formation des placodes sensorielles, de l'oreille interne et des nageoires pectorales, en plus de diminuer la pigmentation et de perturber sévèrement le développement de la queue et du repli médian de la nageoire. Parallèlement, une diminution de l'expression de Parp3 conduit à une augmentation massive de la mort cellulaire par apoptose. J'ai aussi fait le « knock-down » de Parp1 et Parp2 chez le poisson-zèbre. Les résultats suggèrent que la fonction de Parp1 est différente de Parp3 chez le poisson-zèbre tandis que les données concernant Parp2 ne sont pas conclusives. Nos travaux démontrent que Parp3 est essentielle très

tôt au cours développement du poisson-zèbre, possiblement en exerçant un rôle sur la régulation de la transcription durant la spécification des bordures de la plaque neurale et en intervenant dans la promotion de la survie cellulaire durant les premiers stades du développement.

Acknowledgments

First, I wish to thank D[r] Marc Ekker who allowed me to join his lab in 2009 and always had faith in me. I have learned very much under his supervision. I would not hesitate to collaborate with him in the future.

I also would like to thank my collaborators. Thanks to D[r] Guy G. Poirier for involving me in the preexisting collaboration with D[r] Ekker and Vishal Saxena. Thanks to D[re] Michèle Rouleau who was of paramount assistance during the course of this thesis. She inspired me and provided me support and guidance, even though a considerable distance separated us from working side by side.

Special thanks to Vishal Saxena who introduced me to many molecular techniques and accompanied me during less prosper times. You are a friend and working with you was a great pleasure. Thanks also to D[re] Mélanie Debiais-Thibaud for her generous help in troubleshooting protocols.

Finally, I want to thank D[re] Marie-Andrée Akimenko for her advices in general and also for her help concerning fin development.

Statement of contributions

I performed and analysed all the experiments described in this thesis except for the following:

- Vishal Saxena did the first series of microinjections of *parp3* Morpholino oligonucleotides (MO), including the dose response experiment. I characterized the phenotype of these *parp3* morphants.
- Vishal Saxena injected the *parp3* MO and performed the in situ hybridization (ISH) with the *sox9a*, *dlx3b* and *dlx4b* probes. I analysed the results.
- Vishal Saxena did the microinjections of *parp3* MO in the two following transgenic lines: Tg(fli1:EGFP) and Tg(2,4shh:GFPABC15).
- D^{re} Michèle Rouleau (Dr. Guy Poirier's laboratory) performed the immunoblots and poly(ADP-ribose) activity blots on morphant and control embryos that I had produced.

1 Introduction

1.1 Poly(ADP-ribosyl)ation

In 1966, Chambon and his colleagues identified a homopolymer of ADP-ribose. With the addition of nicotinamide adenine dinucleotide (NAD^+) to liver nuclear extracts they demonstrated that this homopolymer enclosed 2 mol of ribose and 2 mol of phosphate per mol of adenine and that the hydrolysis of (NAD^+) was required to synthetize the poly(ADP-ribose) (pADPr) (Chambon et al., 1966). pADPr is a posttranslational protein modification conjugated to the lateral chain of glutamic acids (Riquelme et al., 1979; Burzio et al., 1979) or lysine (Messner et al., 2010). The branched ADPr homopolymer catalyzed by the enzyme can reach 200 to 300 ADPr residues (Miwa and Sigumira, 1984). The polymer is a transient structure that is synthesized by poly(ADP-ribose) polymerases (PARP) and the enzymes responsible for the pADPr catabolism are pADPr glycohydrolase (PARG) and the ADP-ribosyl protein lyase. PARG possesses an exoglycosidase activity and an endoglycosidase activity while the activity of ADP-ribosyl protein lyase is only to hydrolyse the most proximal unit of ADPr on the protein acceptor reviewed by (D'Amours et al., 1999; Rouleau et al., 2004). For visual see figure 1.1.

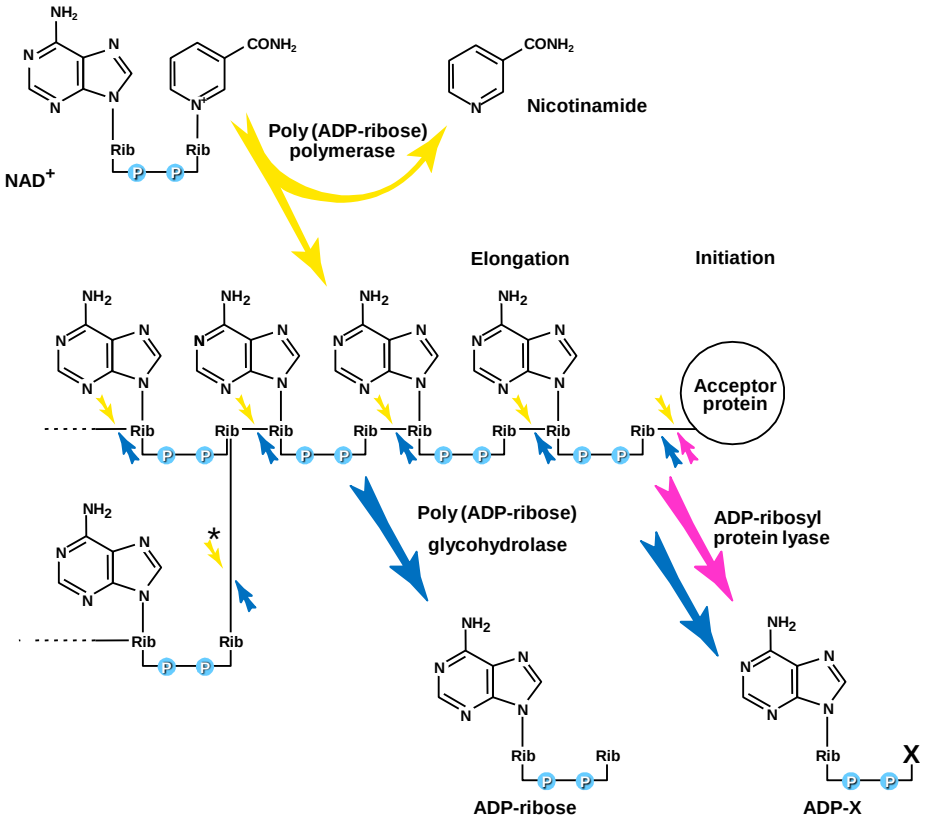

Figure 1.1 Metabolism of poly(ADP-rybosyl)ation. Poly(ADP-ribose) polymerases (PARP) use NAD^+, with subsequent release of nicotinamide, to catalyze the transfer of ADP-ribose (ADPr) onto acceptor protein substrates (the initiation) and the polymerization of ADPr units by making glycosidic bonds between the residues (elongation). The ADPr chain can reach hundreds of residues. Branching "*" is catalyzed only by PARP1 and PARP2 so far (Hottiger et al., 2010). Glycosidic bonds are broken by the exoglycosidic and endoglysodic activities of the poly(ADP-ribose) glycohydrolase (PARG). The most proximal ADPr is released either by PARG (Desnoyers et al., 1995)

or by the ADP-ribosyl protein lyase (Oka et al., 1984). Yellow arrows represent the activities of PARPs while blue and pink arrows represent PARG and ADP-ribosyl protein lyase respectively. This figure was produced by the author of this thesis.

1.2 Poly(ADP-ribose) polymerase 1

PARP1 is the most studied member of the PARP family, which comprises 17 members (Otto et al., 2005) and is able to synthesize polymers of ADP-ribose like 4 other members (Kleine et al., 2008; Hottiger et al., 2010). For more than a decade, it was though that it was the sole enzyme capable of doing such reaction until the discoveries of 4 more at a time of press (see below). The PARP1 organization domains was first characterized by Nishikimi and Kameshita in early 1980s. They identified the protein as a multifunctional enzyme containing three distinct domains: a DNA-binding domain (DBD), an automodification domain and a catalytic domain. In the late 1980s, the nucleotide sequence of the human PARP (hPARP1) was cloned (Cherney et al., 1987) and facilitated the characterization of its biological function. hPARP1 is a 113kDa protein that binds tightly to DNA strand breaks via its two zinc finger motifs from the DBD domain and afterwards auto-poly(ADP-ribosyl)ates on to glutamic residues of its automodification domain, consequently modifying the protein structure enough to cause its release from the DNA which in return allows access to repair enzymes (Satoh et al., 1992). It is likely that the addition of negatively charged phosphate backbone from ADPr is repulsing the DNA. Since it was the first PARP to be cloned and characterized, the protein was named PARP1. The nuclear enzyme is very abundant (Yamanaka et al., 1988), ubiquitously expressed (Schreiber et al., 2002) and is considered the most active PARP being responsible for the major Poly(ADP-ribosyl)ation within the cells in response to DNA strand breaks. Indeed, pADPr synthesis is directly proportional to the amount of single strand breaks (SSB) and double strand breaks (DSBs) present in the genomic DNA within a living cell (Althaus et al., 1987). Furthermore, studies using mice deficient in PARP1 revealed that PARP1 is responsible for about 90% of pADPr synthesis in

response to DNA strand breaks (Shieh et al., 1998; Amé et al., 1999). However, the second study also revealed the existence of other poly(ADP-ribosyl)ating enzymes (see below).

Several nuclear proteins involved in the modulation of chromatin structure have been identified to be covalently modified by PARP1 in vivo. Histones, members of the high mobility group proteins (HMG), topoisomerases I and II, PARP1 and 2 as well as lamins are nuclear acceptors proteins reviewed in (D'Amours et al., 1999; Rouleau et al., 2004; Hassa et al., 2006). Poly(ADP-ribosyl)ation of histones is associated with chromatin decondensation (Poirier et al., 1982). The modulation of chromatin structure is not the sole role attributed to PARP1 as many studies revealed that PARP1 is associated with DNA repair, transcription, replication and recombination with all of these involvements supported by the fact that PARP1 has acceptor proteins in each of these categories, reviewed by (D'Amours et al., 1999). DNA repair remains one of the most active area of research given that poly(ADP-ribosyl)ation mediated by PARP1 accelerates DNA damage repair and the given success of PARP inhibitors for cancer therapy (Haince et al., 2005; Yelamos et al., 2011).

1.3 The PARP family

After more than 10 years focussing on the characterization of a single PARP protein, five new genes encoding proteins with a PARP catalytic domain were discovered; *PARP2* (Amé et al., 1999), *PARP3* (Johansson, 1999), *PARP4* (vPARP) (Kickhoefer et al., 1999), *PARP5a* (Tankyrase1) (Smith et al, 1998) and *PARP5b* (Tankyrase2) (Kaminker et al., 2001). All of them comprise a common catalytic domain similar to the 40-kDa of the C-terminal catalytic domain of PARP1 (Ruf et al., 1998), including the nicotinamide binding cleft responsible for the transfer of

ADP-ribose on acceptors proteins. Currently, the conserved catalytic region is referred to as the PARP signature (Amé et al., 2004). An *in silico* study based on human EST sequences (Otto et al., 2005) suggested that as many as 17 proteins may belong to the PARP family. However, a subsequent study revealed that only PARP1, PARP2, PARP3, vPARP, Tankyrase1 and Tankyrase2 are "true" PARPs, being able to build ADP-ribose polymers or oligomers, while the other putative PARPs identified are only capable of mono-ADP-ribosylation (Kleine et al., 2008; Hottiger et al., 2010). Because not all PARPs possess a polymerase activity the International Union of Biochemistry and Molecular Biology (IUMB) proposed a new nomenclature for all proteins catalyzing the transfer of ADP-ribose onto acceptor proteins as ADP-ribosyltransferases (ARTs) with a D extension for PARP-like ARTs because they are related to the mono-ADP-ribosyltranferase from Diphteria toxin (Hottiger et al., 2010), which, in fact, was the first ART enzyme discovered (Collier and Pappenheimer, 1964). For the purpose of this thesis, the ancient PARP nomenclature will be used given that the focus is on the three following polymerases: PARP1, PARP2 and especially PARP3.

1.4 PARP1 and PARP2 have redundant functions

PARP2 is 62kDa nuclear protein (Amé et al., 1999) having the catalytic domain with the highest similarity to that of PARP1, that is 69% (Olivier et al., 2004). However there are some differences in terms of other domains (Fig 1.2) since PARP2 does not comprise a duplicated zinc finger motif in its DBD despite a highly basic DBD .Neither does it have the BRCT motif, which serves as automodification domain of PARP1. In PARP2, this function is carried by the WGR domain (Amé et al, 1999; Schreiber et al., 2002). PARP2 was first identified by Amé and coworkers as a player in the DNA damage response as it binds to and is activated by DNA strand

breaks. The authors also demonstrated that it encompasses most of the remaining poly(ADP-ribosyl)ation activity within the cell in response to DNA strand breaks. In another study **(**Schreiber et al., 2002), they demonstrated that cells deficient in PARP2 display a similar delay to reseal SSB than cells depleted in PARP1. Furthermore, they showed that PARP2 and PARP1 form heterodimers and poly(ADP)ribosylate each other in vivo. In addition, their study revealed that PARP2 interacts with the following PARP1 targets involved in single strand break repair/base excision repair (SSBR/BER): X-ray repair cross-complementing I (XRCC1), DNA polymerase β and DNA ligase III. Knockout mouse models for *PARP1* and *PARP2* were produced (Ménissier de Murcia et al., 1997; Ménissier de Murcia et al., 2003) and both showed a hypersensitivity to ionizing radiation as they had increased rates of apoptosis due to an accumulation of DNA strand breaks demonstrating their importance in the DNA damage response (DDR). Although no striking evidence of developmental defect was observed in these studies, PARP2 knockout mice revealed defects in spermatogenenis (Dantzer et al., 2006), thymopoiesis (Yélamos et al., 2006) and decreased adipogeneration (Bai et al., 2007) whereas no developmental abnormalities in *PARP1*$^{-/-}$ mice have been found to date. However the targeted deletion of both *PARP1* and *PARP2* (Ménissier de Murcia et al., 2003) results in a lethal phenotype; these mice die during early embryogenesis more specifically at the onset of gastrulation. This result suggests that the two proteins have a compensatory and fundamental role during early development of mammals. Taken together, these studies indicate that PARP1 and PARP2 have redundant functions although slight differences between the two are starting to emerge (Yélamos et al., 2008).

1.5 PARP3

Like PARP2 (62kDa), PARP3 (63kDa) is smaller than PARP1 (113kDa) and does not comprise a DNA binding domain with two zinc finger domains such as PARP1 (Johanson et al., 1999). Although the DBD of PARP3 has not been identified, it has been observed in vitro that PARP3 is able to bind to chromatin and to DNA (Rouleau et al., 2011; Rulten et al., 2011). Hence a putative DBD of PARP3 may remain to be characterized. PARP3 shares with PARP1 and PARP2 a WGR domain upstream of their PARP domain (Fig 1.2).The PARP3 N-terminal domain is 54 amino acid-long only and the catalytic domain comprises 489 amino acids which confers 61% similarity with the human PARP1 catalytic domain (Johanson et al., 1999; Augustin et al., 2003). The human gene encodes two PARP3 isoforms due to alternative splicing of the PARP3 transcripts. A long PARP3 isoform, expressed at low levels, comprises a 7 amino acids extension on its N-terminal side that is absent in the short and predominant isoform (Rouleau et al., 2007). PARP3 function is poorly characterized nevertheless insights are starting to come into place for instance, it was reported lately that PARP3 is essential for the stabilization of the mitotic spindle during mitosis by acting on the mitotic components: NuMa and tankyrase 1 (Boehler et al., 2011). Congruent with the original function of PARP, PARP3 was found to be associated with members of the DNA repair machinery namely: DNA-PKcs, PARP-1, DNA ligase III, DNA ligase IV, Ku70, and Ku80 (Rouleau et al., 2007) suggesting that the protein is also involved to some extent in the response to DNA damage. It has been recently demonstrated that PARP3 is recruited to and stimulated by DNA strand breaks (Boehler et al., 2011; Rulten et al., 2011).Moreover, its presence is necessary for an efficient DSB repair in human cell line following γ irradiation (Rulten et al., 2011). However its contribution in the DNA damage response appears modest according to its activation level seen in this publication and our

knowledge of PARP1 and PARP2 activation (Shieh et al., 1998; Schreiber et al., 2002). PARP3 is conserved among eukaryotes species (Otto et al., 2005) which indicates that regardless of its modest activity the protein probably has an important role. Consequently further research is needed to understand its specific functions.

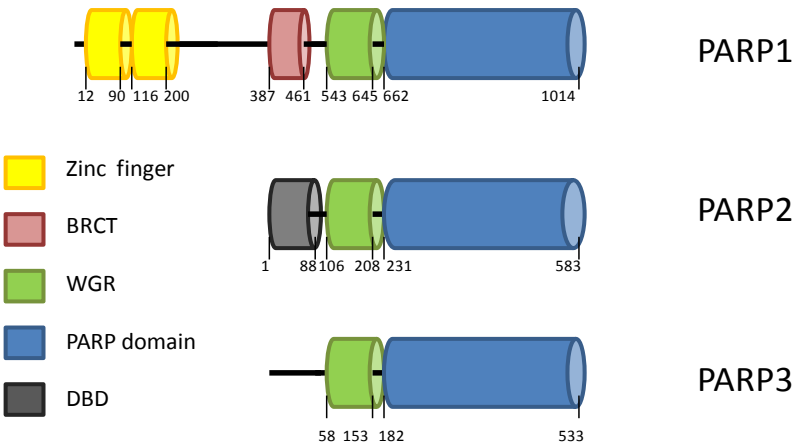

Figure 1.2 Schematic representations of structural domains of human PARP1, PARP2 and PARP3. One isoform per protein is shown. PARP1 accession number is NP_001609 (long isoform), PARP2 accession number is NP_005575 (long isoform) and PARP3 NP_005476 (short isoform). Protein domain sizes are according to NCBI protein data base and UniProt. This figure was produced by the author of this thesis.

1.6 PARP3 is more tightly regulated than PARP1 and PARP2

The subcellular distribution of PARP1 and PARP2 is similar. Indeed they are localized in the nucleus and nucleolus whereas they are not found within the cytoplasm (Meder et al., 2005). The cellular distribution of PARP3 is different because a little fraction of the protein does locate in the cytoplasm even if it most of it accumulates in the nucleus (Rouleau et al., 2009; Rouleau et al., 2011). There are important differences in cell type distribution as well. An immunocytochemical study allowed the establishment of the tissue distribution of PARP3 in *cynomolgous* monkeys, closely related to humans. The first key finding of this study is that, rather than being ubiquitously expressed like PARP1 and PARP2 (Schreiber et al., 2002), PARP3 is only present in a subset of cell types within a given tissue. The second key finding is that the highest expression of PARP3 is in the ductal epithelia of secretory tissues and in neurons of the terminal ganglia (Rouleau et al., 2009). Studies conducted with rodents have shown that PARP1 and PARP2 have significantly higher expression in testis and spermatogenic cells (Concha et al., 1989; Menegazzi et al., 1991; Schreiber et al., 2002). Noteworthy, PARP3 expression is limited to specific cells in the testis namely: the Leydig's cells and the Sertoli cells (Rouleau et al., 2009). In the overall study in *cynomolgous* monkeys, there are evidences that PARP3 is generally more prominent in differentiated cells than in pluripotent or multipotent cells, suggesting a rigid regulation for PARP3 and, possibly, a specific function.

1.7 PARP3 and the epigenetic regulation of transcription

Although the functions of PARP3 are poorly characterized, recent evidences lead to the conclusion that PARP3 may play a role in the development by regulating transcription. First, because PARP3 associates with protein members of the Polycomb group (PcG), it could be an

active player in the epigenetic regulation of development (Rouleau et al., 2007). The maintenance of gene expression, often referred to "transcriptional memory" is very important for the development of the diverse cell types of an organism. Trithorax group (TrxG) and PcG proteins were first described in *Drosophila* as protein groups that modify the state of the chromatin, on and off, respectively, as reviewed by (Francis and Kingston, 2001). These proteins have orthologs in many metazoans including humans, as reviewed by (Levine et al., 2004; Schuettengrube et al., 2007) PcG proteins use a combination of posttranslational modifications and structural changes to the underlying chromatin structure to maintain silenced epigenetic states throughout development, as reviewed by (Levine et al., 2004) In 2007, Rouleau and coworkers found that human PARP3 is associated in part with PcG bodies, as revealed by immunofluorescence microscopy, while immunoprecipitation experiments revealed that PARP3 forms complexes with several Polycomb proteins including the methyltransferase Enhancer of Zeste homologue 2 (EZH2), Suppressor 12 of Zeste (SUZ12), the transcriptional repressor YY1, RbAp46/48, Extra sex comb (ESC) homolog Embryonic Endoderm development (EED) and histone deacetylase 1/2 (HDAC)1/2. Furthermore, they localized hPARP3 with the repressive mark H3K27me3 which is catalyzed by the methyltransferase EZH2 (Rouleau et al., 2007). These observations suggested a function for PARP3 in transcriptional repression which could be important during development. EZH2 and SUZ12 are core components of the PRC2 complex, the class I Polycomb repressor complex (PRC) which is known to be involved in developmental patterning (Levine et al., 2004). Subcellular fractionation of a human cell line showed that PARP3 predominantly accumulates in the nucleus and it associates with the chromatin (Rouleau et al., 2011). It was also demonstrated by immunofluorescence that PARP3 is found in numerous small foci and a few larger foci and that PARP3 is co-localized with the trimethylation of lysine

27 of Histone 3 (H3K27me3) within these foci (Fig. 1.3). Recently, our collaborators found that PARP3 can add ADP-ribose units on EZH2 and SUZ12 (M. Rouleau and G. Poirier, personal communication). Taken together, these results suggest that PARP3 could play an important role in the epigenetic regulation of transcription throughout developmental process by targeting the PRC2 complex.

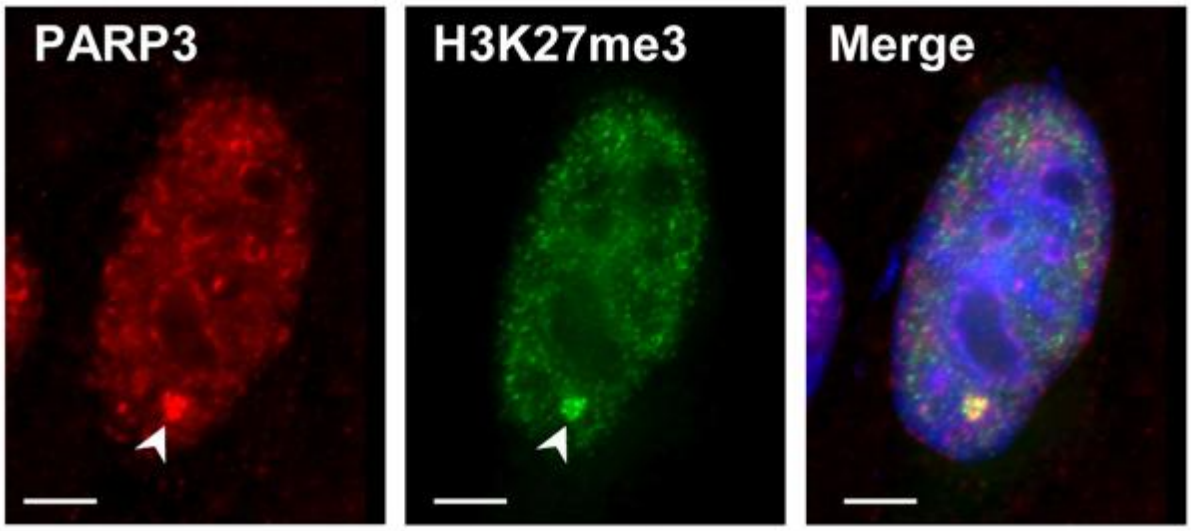

Figure 1.3 PARP3 is found in foci and is associated with the repressive mark H3K27me3. Immunofluorescence detection of PARP3 in SK-N-SH cells. PARP3 is predominantly nuclear and co-localizes with trimethylated histone H3K27 (H3K27me3) (arrowhead). Scale bars represent 3 mm. (Reproduced from Rouleau et al., 2011; with permission)

1.8 PARP3 mostly binds to genes involved in the regulation of development

In addition to a role for PARP3 in the epigenetic regulation of transcription, it appears that PARP3 targets genes involved in development by binding them around their translational start site (Rouleau et al., 2011). Collaborators from the Hôtel-Dieu de Québec (Québec, Canada) carried out an investigation of the genomic occupancy of PARP3 in human SK-N-SH cells to assess the roles of PARP3 in gene transcription. They pulled-down PARP3-associated sequences and conducted a ChIP-chip analysis using a specific PARP3 antibody. They determined that PARP3 was associated with 11% of the genes present on the array, a percentage similar to the gene occupancy by other members of the PRC2 complex (Lee et al., 2006; Bracken et al., 2006). Genes in the vicinity of PARP3-bound sequences were classified according to their biological processes using Gene Ontology (GO) annotations. This analysis revealed a remarkable enrichment of PARP3 around developmental genes (Fig. 1.4A). Many of these encode homeobox transcription factors regulating early specification events, including genes of the HOXC cluster, several members of the SOX, FOX, DLX, IRX families, as well as numerous genes encoding basic helix-loop-helix (bHLH) transcription factors (Fig. 1.4B). Collectively, these genes regulate axial and tissue patterning, cell fate specification, craniofacial development, and neurogenesis. The ChIP-qPCR analyses (conducted independently from ChIP-chip experiments) revealed a significant and important enrichment of PARP3 on the majority of the selected genes relative to their enrichment after control ChIP with rabbit IgG. Maximal enrichment was observed around genes encoding the neurogenic differentiation 2 (NEUROD2), NK2 homeobox 1 (NKX2.1), in the coding region of the distal-less homeobox 3 (DLX3) gene and in proximity of the sex determining region-Y box 9 gene (SOX9) (Fig.1.5 A). This set of data confirms that PARP3 does specifically bind developmental genes and in particular some crucial for neuronal

specification. Furthermore, PARP3 targets overlapped remarkably with SUZ12 and H3K27me3 targets (Fig.1.5B), even though SUZ12 and H3K27me3 bound genes were established in different cell lines (Bracken et al., 2006). These observations strongly support an association between PARP3 and PRC2, and suggest that they could transcriptionally co-regulate developmental genes.

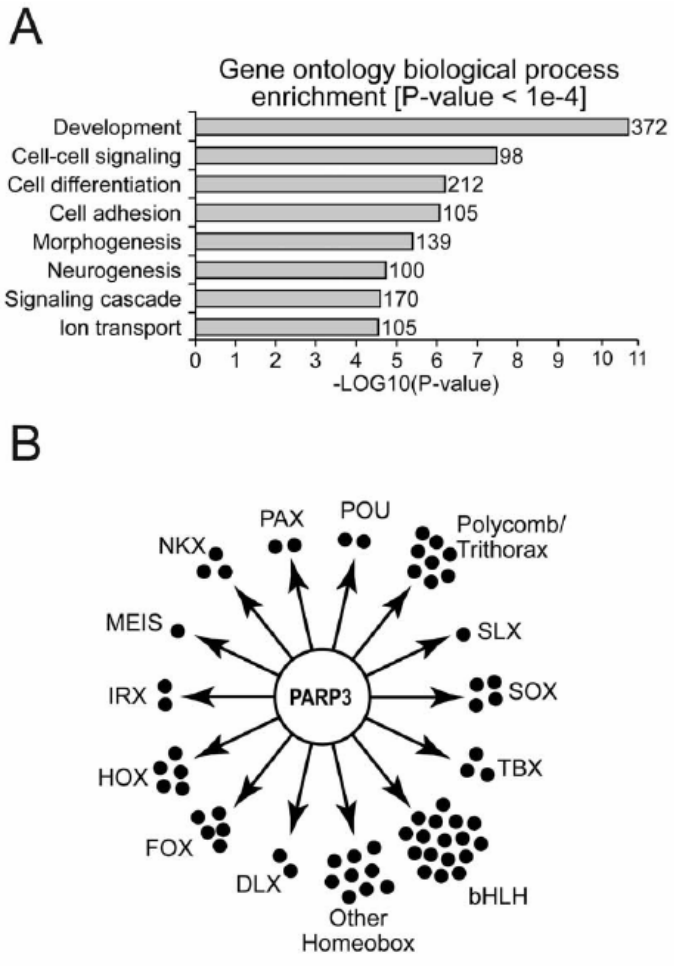

Figure 1.4 PARP3 targets developmental genes. A. Enrichment of PARP3 targets according to gene ontology annotations. B. Families of development-related transcription factors targeted by PARP3, as identified by ChIP-chip analysis. Rabbit IgG were used for the control ChIP. (Reproduced from Rouleau et al., 2011; with permission)

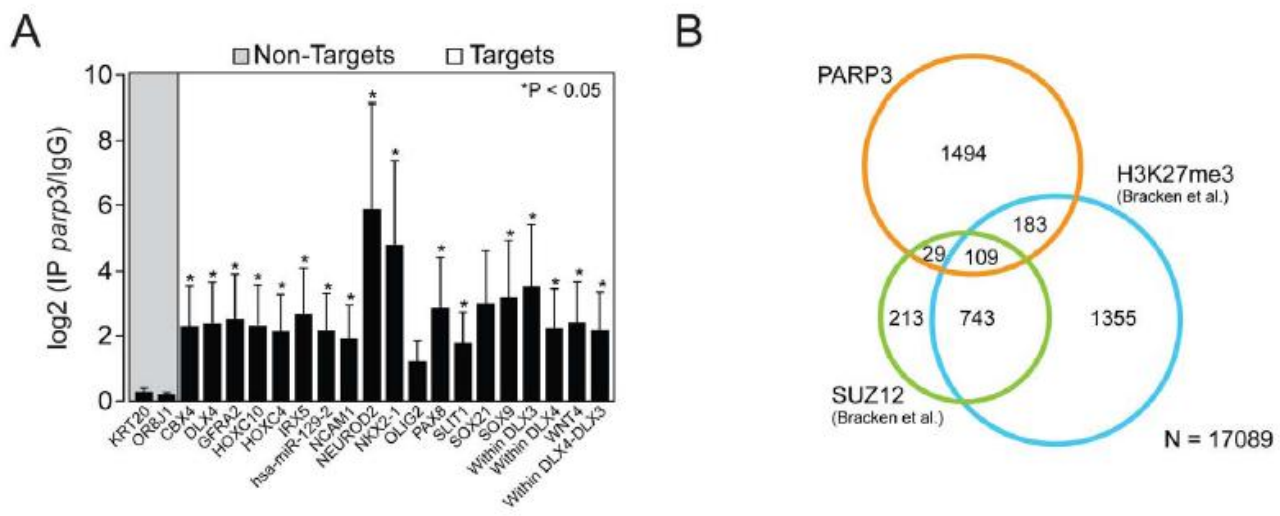

Figure 1.5 Analysis of PARP3-bound targets. A. Validation of PARP3 developmental targets by ChIP-qPCR. PARP3 ChIP were analyzed by standard qPCR using primers specific for regions targeted by PARP3 according to ChIP-chip results. Error bars represent the standard deviation from three independent experiments and asterisks indicate a significant enrichment relative to control (p,0.05). Two control regions (KRT20 and OR8J1), which are not bound by PARP3 (Non-targets), were used to determine basal signal. Several probes were used for DLX genes. The ‘‘DLX4’’ probe targets the promoter region, ‘‘within DLX’’ probes target sequences within the DLX genes and ‘‘within DLX3-DLX4’’ probe targets the DLX3-DLX4 intergenic region. B. Overlaps between PARP3 and SUZ12 targets or sequences enriched in H3K27me3. SUZ12 and H3K27me3 targets were those determined in human embryonic fibroblasts by (Bracken et al., 2006). (Reproduced from Rouleau et al., 2011; with permission)

1.9 PARP3 expression is altered in neuroblastoma

Neuroblastoma (NB) is a type of tumour that develops in various sites of the peripheral nervous system (Jiang et al, 2011). It is the most frequent extracranial solid tumour in children and accounts for 15% of paediatric cancer death (Maris et al., 2007). Among non familial NB there are different chromosome irregularities caused by chromosomal deletions or aberrant chromosomal rearrangements (Jiang et al., 2011). *PARP3* is located in the chromosomal region 3p21, which is often lost in the poor prognosis 11q genetic subtype of stage 4 NB (Hoebeeck et al., 2007; Nair et al., 2007). Of note, the loss of the long arm of chromosome 11 is the second most frequent deletions in NB (Jiang et al., 2011) meaning that the non-expression of PARP3 is frequent in neuroblastoma. For this reason, it is possible that PARP3 is acting as a tumour suppressor in NB. This type of tumour develops from neural crest cells (NCC) (Brodeur et al., 2003; Maris et al., 2007). NCC are derived from the original ectoderm during gastrulation and they persist into late organogenesis. They are first specified at the beginning of neurulation, a process that conduct the formation of the neural tube, where they are located between the neural ectoderm and non-neural ectoderm (epidermis) (Fig.1.6). Pre-migratory neural crest cells exert cell-cycle control and maintain their multipotency all along this process. NCC delaminate from the surrounding cell layers at the closure of the neural tube and then emigrate to reach different areas that will determine their fates, including cells of the peripheral nervous systems (Sauka-Spengler and Bronner-Fraser, 2008). Given that *PARP3* seems to be involved in the regulation of transcription during development as well as being involved in DSBs, we hypothesized that PARP3 is an important player in the control of transcription and in the maintenance of genomic integrity of NC cells and that these PARP3-dependent mechanisms are altered in NB.

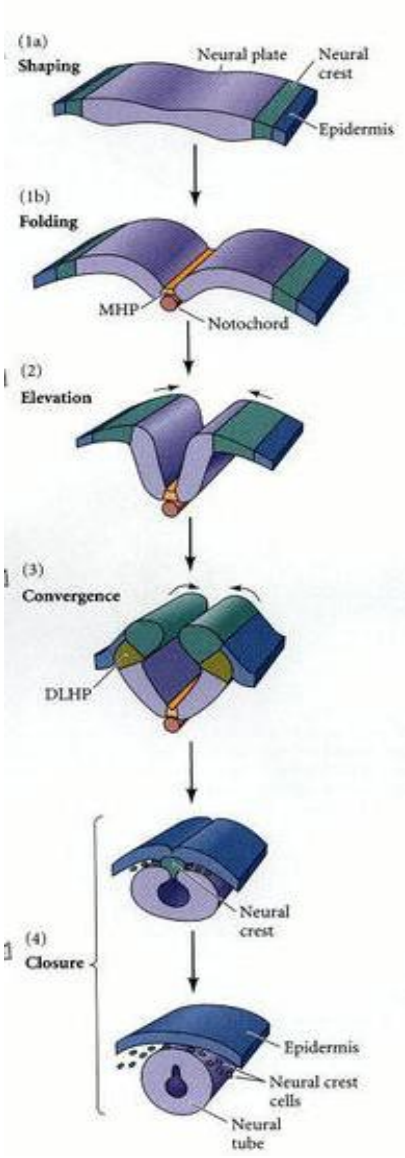

Figure 1.6 Neural crest formation occurs during neurulation.

(1a) Cells of the neural plate are elongating and then (1b) the neural plate folds as the medial neural hinge point (MHP) cells anchor to the notochord, while the presumptive epidermal cells move toward the dorsal midline. (2) The neural folds are elevated as the presumptive epidermis continues to move toward the dorsal midline (3) Convergence of the neural folds occurs as the dorsolateral hinge point (DLHP) cells become wedge-shaped and the epidermal cells push

toward the center. (4) The neural folds are brought in contact with one another, and the neural crest cells link the neural tube with the epidermis. The neural crest cells detach and emigrate, leaving the neural tube separate from the epidermis. (Reproduced from Gilbert S. F, 2006; with permission)

1.10 Neural crest is a common feature to vertebrata

The development of vertebrates involves complexities that are not established in "lower" organism. Although, vertebrates are traditionally characterized by the presence of a vertebrate column, the transient neural crest cell layer is considered as an evolutionary novelty that differentiates them from the other deuterostomes especially because of its derived craniofacial structures (Wilkie and Morriss-Kay, 2001). It was also suggested to be the fourth germ layer, which renders vertebrate quadroblastics (Hall et al., 2000). The gene machinery that is responsible for the key steps in the NCC formation is thought to be relatively similar in all vertebrates (Sauka-Spengler and Bronner-Fraser, 2008). Consequently we have used a vertebrate animal model to study the role of PARP3 in the developing embryo and its relationship with the neural crest.

1.11 The zebrafish, *Danio rerio* as a model for studying consequences of Parp3 loss of function

The zebrafish is a widely used model for developmental biology studies given that the development of the embryo and of the larvae are very well characterized (Kimmel et al., 1995). It is relatively easy to identify both embryonic and larval stages because they are well defined but also because embryos are optically clear (Kimmel et al., 1995), a feature that facilitates the observation of developmental defects since we can see internal structures. Other excellent reasons to work with this model are: the rapid growth, the short generation time and a large progeny which can be more than 100 embryos per couple (Westerfield, 2000). Finally, it is possible to downregulate specific genes by microinjection of anti-sense morpholino oligonucleotides (Nasevicius and Ekker, 2000). In addition to all these features, the genome of

the zebrafish comprises *parp1*, *parp2* and *parp3* genes orthologous to their respective human genes. The Parp3 sequence is very well conserved and hence zebrafish is a good model for our studies. Based on an analysis of EST sequences, the zebrafish genome, similar to the mouse genome, appears to code only for the short isoform (Fig.1.7).

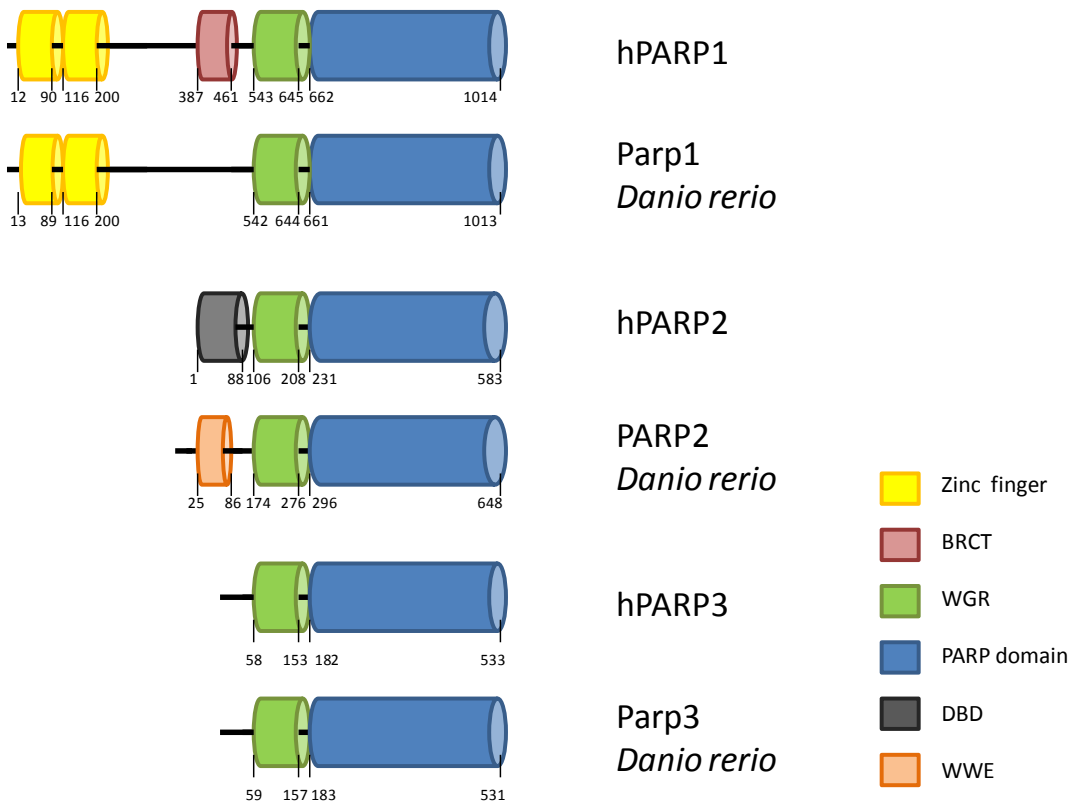

Figure 1.7 Schematic representations of structural domains of human (h) PARP1, PARP2, and PARP3 compared with their zebrafish (*Danio rerio*) orthologues. One isoform per protein is shown. hPARP1 accession number is NP_001609 (long isoform), hPARP2 accession number is NP_005575 (long isoform) and hPARP3 NP_005476 (short isoform) while zebrafish Parp1 is NP_001038407, zebrafish Parp2 is NP_001191199 and zebrafish Parp3 is NP_956795. Protein domain sizes are according to NCBI protein data base and UniProt. This figure was produced by the author of the thesis.

1.12 Statement of inquiry

The biological function of PARP3 is poorly defined compared to that of PARP1 and PARP2. Its catalytic activity has been described as well as its structure but only a few recent clues about its physiological role were reported. Some of the new data about the putative roles of PARP3 were published during the course of this thesis (Boehler et al., 2011; Rulten et al., 2011). Furthermore, there are diverse indications that PARP3's function is indeed different from those of PARP1 and PARP2. We thus aimed to better describe the biological function of PARP3. Given that *PARP3* seems to be involved in the regulation of transcription during development, especially that of transcription factor genes, as well as being involved in DSBs, we hypothesized that PARP3 is an important player in the control of transcription and in the maintenance of genomic integrity of NC cells and that these PARP3-dependent mechanisms are altered in cancer-derived of neural crest cell, namely neuroblastoma. We have chosen the zebrafish as a vertebrate animal model because most of the targets identified as PARP3-bound genes were transcription factors involved in development and also, the zebrafish is a good animal model in the field of development biology. Importantly, the amino acid sequences of human PARP3 and zebrafish Parp3 are very similar. Our first objective was to determine the effect of Parp3 loss of function in zebrafish. Consequently we have used the technology of anti-sense morpholino oligonucleotides (MO) to knockdown the expression of *parp3* thereby allowing us to observe the consequences of Parp3 depletion in developing embryos and young larvae. Our second objective was to investigate if Parp3 loss of function would cause expression pattern impairments for the transcription factors previously identified as PARP3-bound genes in humans. We thus used in situ hybridization to look at the expression of some of these genes, in zebrafish embryos, following knockdown of *parp3*. Moreover we sought to verify whether the neural crest cells were affected in these

embryos given that transcription factors primordial in inducing early differentiation programs of neural crest progenitors were significantly bound by PARP3 in the ChIP-qPCR validation experiment. The third objective was to survey the apoptosis of zebrafish embryo with impaired Parp3 expression since PARP3 responds to DNA damage by increasing the efficiency of DNA repair. My objective was to address whether the maintenance of genomic integrity is dependent on Parp3 and whether this mechanism is neural crest specific? The last objective was to look at the function of Parp1 and Parp2, in zebrafish, by producing embryos with a MO-mediated depletion of Parp1 and/or Parp2.

2 Materials and methods

2.1 Zebrafish husbandry

Embryos were obtained from in-house breeding of adults obtained at a local pet store and maintained using published methods. All experiments were performed according to the guidelines of the Canadian Council on Animal Care and were approved by the University of Ottawa animal care committee (permit number BL-249). Adults were placed in breeding tanks from aquatic habitats the day before being bred and separators were removed between 9 to 10 o'clock in the morning of injection. Zebrafish embryos and larvae (up to 6 days) were grown at 28.5 ^{o}C with E3 embryo media. Embryos that were used for *In situ* hybridization or for Sirius red staining were grown in E3 embryo media that contained 0.2 mM *propylthiouracil* (PTU).

2.2 Microinjections of Morpholino oligonucleotides (MO)

Morpholino oligonucleotides (MO) complementary to the translational start site of the zebrafish *parp3* (MO1) and to the sequence immediately upstream of the translational start site of *parp3* (MO2) had the following sequences: MO1: [5'ATGCTGCCCTTCTCTTGGGTGCCAT], MO2: [5'CTTTGTCCTCTGATACTGGCGGTAC].The *parp1* MO sequence was: [5'CTTGTCGTCCTGTGAGTCGGCCATC] and the *parp2* MO: [5' CCCTGCAACTCC TTGTTCGTCGCAT]. A non-targeting MO and a *p53* MO used as controls had the following sequences: [5'CCTCTTACCTCAGTTACAATTTATA] [5'GCGCCATTGCTTTGCAAGAA ATTG], respectively. All MOs were obtained from Gene Tools Inc. MOs were solubilised in autoclaved ddH_2O and stored at room temperature. Prior to injection, MOs were diluted in Danieau buffer (4 mM $MgSO_4$; 6 mM $CaCl_2$; 7 mM KCl; 580 mM NaCl; 50 mM Hepes, pH 7.6)

to a final concentration of 10X and 0.5% phenol red were added to a final concentration of 10X. All embryos were microinjected at the one-cell stage with 1 nL of MO preparation using an IM 300 microinjector (Narishige). A Needle was calibrated once by injecting into mineral oil droplet on a calibrating slide and the volume of the air bubble was calculated. Afterwards, the other needles were cut following this calibrated needle. For the dose-response experiments (Fig. 2.2D), 1 nL of *parp3* MO were at the following concentrations: 0.25 mM (2 ng), 0.5 mM (4 ng), and 1.0 mM (8 ng). A concentration of 0.5 mM (4 ng) of *parp3* MO was microinjected for all other experiments. The *p53*MO (0.5 mM) was microinjected alone or co-microinjected with *parp3* MO1 (0.5 mM). The *parp3* MO was also injected into embryos from the following 3 transgenic lines: Tg(fli1:EGFP), Tg(2,4shh:GFPABC15) and Enhancer trap 37 (ET37) (all kindly given by Dr M-A Akimenko, U of Ottawa). The Microinjections of *parp1* MO and *parp2* MO were performed with 0.5 mM (4 ng), 0.75mM (6ng) and 1.0 mM (8 ng) for each MO. The *p53*MO (0.75 mM) was microinjected alone or co-microinjected with *parp1* MO (0.75 mM).

2.3 Staging the zebrafish embryos and larvae

Stage evaluations were done by applying criteria outlined by Kimmel et al., 1995. Thus, at the proper time after birth, embryos were evaluated for specific characteristics and collected when they reached those standard characteristics. For example, the 10 hpf stage corresponded to embryos that demonstrated 100 % epiboly. Embryos staged as16 hpf were characterized by a constriction at the posterior region of the yolk that gives to the yolk a typical kidney bean shape. For 24hpf, we were looking for a heartbeat. Finally, wt 48hpf were characterized by pectoral fin buds that curve into the posterior direction. To stage the *long-pec stage* (48hpf) of embryos

injected with the *parp3* MO, we collected morphant embryos at the same time as control embryos from the same clutch as no pectoral fin buds develop in the morphants.

2.4 RNA production

FLAG-PARP3 RNA was produced with the linearized construct pT7TS-FLAG-shPARP3 previously produced by Dr M. Rouleau (CHUL, Québec). The construct was linearized with the restriction enzyme *Sst1* and subsequently verified by electrophoresis on a 1% agarose gel using GeneRuler DNA ladder (Fermentas). The mMessage mMachine (Ambion) that contained a SP6 RNA polymerase was used for the synthesis of capped RNA. The linearized DNA construct was purified prior to RNA synthesis as well as after the synthesis by adding an equivalent volume of phenol and chloroform both followed by 13500 *x g* centrifugation. DNA and RNA were precipitated by 13500 *x g* centrifugation in 0.3M NaOAC and 0.4M LiCl respectively.

2.5 Preparation of the embryos for immuno or activity blots analysis

Larvae were dechorionated manually with forceps at 48hpf and were euthanized with 50 % tricaine® solution. Afterwards, they were rinsed twice for 2 minutes in cold embryo media and twice for 2 minutes in cold Ringer's solution. Larvae were kept on ice until the yolk was mechanically removed by sucking out the yolk sac with a pipette. Ten to 15 larvae were deyolked in cold Ringer's solution containing 1mM EDTA and 0.3 mM PMSF. The solution was removed and larvae were frozen in liquid nitrogen and stored at -80^{o} C until the protein extraction process. Embryos were shipped to Dr Guy Poirier's lab (University Laval, Quebec city) on dry ice.

2.6 Immuno blots and poly(ADP-ribose) polymerase activity

Frozen embryos were resuspended in Laemmli sample buffer (62 mM Tris-HCl, pH 6.8; 10% glycerol; 2% SDS; 715 mM β-mercaptoethanol; 0.001% bromophenol blue) containing 4 M urea. Embryos were sonicated 3 x 15 sec using the microtip of a Sonic Dismembrator 550 (setting at "3"; Fisher Scientific) and were then heated at 65° C for 15 min. Whole embryo extracts were clarified by a centrifugation at 13 000 rpm for 15 minutes in a refrigerated microcentrifuge (4°C). Clarifed extracts corresponding to a specific number of embryos (as stated in legends to figures in the Results section) were loaded on 8% polyacrylamide gels.

For detection of parp3 and FLAG-PARP3 by Western blot, proteins were transferred onto a 0.45 μm Immobilon-P (PVDF) membrane (Millipore) in transfer buffer (25 mM Tris, 192 mM glycine, 20% methanol), for 1 hour at 4°C using constant voltage (90V) in a MiniProtean transfer cell unit (BioRad). The membrane was subsequently blocked in Phosphate buffered saline (PBS) containing 0.1% Tween-20 and 5% skim milk for 1 hour at room temperature, incubated overnight at 4°C in PBSMT containing a rabbit polyclonal anti-human PARP3 antibody (dilution 1:5000; ALX-210-541, Enzo Life Sciences) or monoclonal anti-mouse FLAG antibody (dilution 1:5000; M2, Agilent), washed 4 x 15 min. in PBSMT. The membrane was subsequently incubated with a goat anti-rabbit antibody conjugated to horseradish peroxidase (dilution 1:5000; Jackson Laboratories) then washed twice in PBSMT and 4 times with PBS containing 0.1% Tween-20. Detection was accomplished using Western lightning Plus-ECL (Perkin Elmer) and Fuji Super RX films.

For poly(ADP-ribose) polymerase activity blots, polyacrylamide gels were incubated for 1 hr at 37°C in electrophoresis buffer (25 mM Tris, 192 mM glycine, 0.1% SDS) containing 0.7 M β-mercaptoethanol. Gels were then equilibrated for 5 min in transfer buffer and proteins were transferred to Immobilon–P as described above. Subsequent steps were conducted by incubation of the membrane at room temperature with gentle rocking. Proteins were renaturated by incubating the membrane in renaturation buffer (50 mM Tris-HCl, pH 8.0; 10 mM NaCl; 0.3% Tween-20; 1 mM DTT) containing 20 μM zinc acetate, 2 mM $MgCl_2$ and 2 μg/ml activated DNA (Sigma) for 1 hour. The membrane was then incubated in the same buffer supplemented with NAD^+ (100 μM; Sigma) for 1 hour to allow pADPr synthesis. Subsequently, unincorporated NAD^+ was washed off by incubating the membrane in the renaturation buffer (without DNA, NAD, Zn acetate and $MgCl_2$), 4 times for 15 min. and then 4 more 15 min. Washes in SDS buffer (50 mM Tris-HCl, pH 8.0; 1 mM NaCl; 1 mM DTT; 2 % SDS). Detection of pADPr synthesis was done as described above for PARP3 using the specific rabbit polyclonal anti-pADPr antibody 96-10 produced in Dr. G. Poirier's lab (Affar et al., Biochimica Biophysica Acta, 1999).

2.7 Probes preparation for whole mount in situ hybridization (ISH)

Anti-sense RNA probes for the following zebrafish genes: *nkx2.1a* (NM131589), *neurod* (NM130978) and *crestin* (AF195881) were produced as follows. Plasmids were linearized at 37 °C with restriction enzymes and precipitated prior to probes synthesis. The linearized DNA was verified by gel electrophoresis by loading the DNA on 1% agarose gel using GeneRuler DNA ladder (Fermentas). To synthesize probes conjugated with digoxigenin-UTP, 1μg of each linearized DNA was incubated at 37 °C for 1 hour with digoxigenin-UTP with the DIG RNA

labelling mix (Roche), buffer (Roche), recombinant RNaseOut (Invitrogen) and T3 or T7 RNA polymerases (Roche). T3 and T7 were chosen according to the orientation of the DNA in the plasmid in order to synthetize anti-sense RNA probes. After a 1-hour incubation, 1µl of recombinant DNase1 (Roche) was added to the sample and incubation was resumed for 15 min at 37°C to digest DNA templates. The products were precipitated twice by incubation overnight at –20 °C with 0.4 M LiCl and 3 volumes of 100% ethanol followed by a 30 minutes centrifugation 13500 *x g* at 4 °C, washed with 70% ethanol DEPC-treated water with subsequent centrifugation and finally, the probes were resuspended in DEPC-treated water. Probes integrity was verified by electrophoresis on a 1% agarose gel using the RiboRuler RNA ladder (Fermentas). The probes and the ladder were heated at 65 °C in a water bath and chilled on in ice for 2 min prior to being loaded on an agarose gel. The concentrations of the probes were measured using NANODROP 2000 spectrophotometer (Thermo scientific).

2.8 Whole mount in situ hybridization

Whole mount in situ hybridization (ISH) was performed with control and *parp3* morphant embryos collected at 10, 16 and 24 hpf. Overall, the ISH protocol was inspired from Thisse and Thisse 2007. Embryos were fixed in 4% paraformaldehyde (PFA) in phosphate-buffered saline (PBS) at 4 °C overnight or for the week end followed by dehydration in methanol 100% and stored at -20°C until used. The following steps carried out over 3 days. The first day consisted in the rehydration of the embryos with phosphate buffered saline and 0.1% Tween-20 (PBT) using methanol series, digestion with10µg/ml proteinase K at room temperature for 45 sec (10hpf), 3 min (16hpf) and 10 min (24hpf) and fixation in 4% PFA in PBS for 20 min. For probe hybridization, embryos were incubated in Hybe mix with tRNA for 3 hours at 65°C. Afterwards,

probes were denatured at 65°C for 10 min just before the embryos were transferred in Hybe mix containing approximately 50 ng of probe for about 20 embryos. The second day, embryos were progressively transferred in 2X SSC (1,75% NaCl, 0,88 % of citric acid trisodium salt in autoclaved water) using series of washes with Hybe mix at 65°C and reintroduced in PBT by a series of washes in 0.2X SSC. Embryos were then incubated for 1 hour in blocking solution (10% calf serum, 40mg/ml bovine serum albumin (BSA) in PBT) prior to incubation with an anti-Digoxigenin antibody conjugated to alkaline phosphatase (anti-Dig-AP, 1:1000). Incubation was performed overnight at 4°C. The third day, embryos were washed 6 to 8 times with PBT before the staining process with AP buffer (100nM Tris HCl, pH 9.5; 50mM $MgCl_2$; 100mM NaCl; 0.1% Tween-20), Nitro blue tetrazolium (NBT-175µg/ml) and 5-bromo-4chloro-3indolyl phosphate (BCIP-225µg/ml). The staining was stopped by transferring the embryos in a 1mM EDTA in PBT solution and a 20 min of post-fixation followed. Embryos were progressively transferred in 100% glycerol prior to photography.

2.9 Acridine orange staining

Control and *parp3* morphant embryos, collected at 24hpf (about 30 of each), were incubated alive with 0.01mg/ml of acridine orange (Sigma) in E3 embryo media for 30 minutes at room temperature and then washed 3 times for 10 min with embryo media. Embryos were anesthetized by an incubation in embryo medium with 6% tracaine® and observed under a dissecting microscope equipped for fluorescence detection using a filter with excitation 480/40., Embryos were light-protected during all steps with aluminum foil until they got exposed to the UV light. Photographs were acquired using a Nikon digital camera.

2.10 Picro-Sirius red staining

This experiment was performed on 48hpf larvae for wt and *parp3* morphants (about 25 larvae each). They were fixed in 4% paraformaldehyde (PFA) in phosphate-buffered saline (PBS) at 4 ^{o}C overnight followed by dehydration in methanol 100% and stored at -20^{o}C until the of staining process. Larvae were rehydrated in PBT using a methanol series until reaching 100 % PBT and stained with 0.1% Sirius red in a saturated picric acid solution for 1 hour. Larvae were washed with ddH_2O until the water ran clear. Larvae were transferred in 25% glycerol in PBT, and mounted between a slide and a cover slip prior to photography.

2.11 Whole mount immunostaining

About 25 *parp3* morphants as well as controls were collected at 24hpf for this experiment. They were mechanically removed from their chorion as described above and fixed in 4% PFA overnight at 4^{o} C. Embryos were washed twice in PBT an incubated for 3 hours in a blocking PBS solution containing 0.5% TritonX-100, 4% calf serum and 1% dimethyl sulfoxide (DMSO) and then washed twice in PBT. Incubation was carried out overnight at 4^{o}C with 1:200 anti-synaptic vesicle glycoprotein 2 (sv2), kindly given by Dr. M. Jonz (U. of Ottawa). Incubation at room temperature with goat anti-mouse antibody (Alexa, 594 red) diluted 1:100 in PBS and followed by 2 washes in PBT. Starting with the secondary antibody incubation, all steps were light-protected with aluminum foil until the samples were exposed to the UV light.

3 Results

3.1 Parp3 is well conserved in zebrafish

The short isoform of human PARP3 and the zebrafish Parp3 were aligned (Fig.2.1). Overall, zebrafish Parp3 shares 71% sequence similarity with the human PARP3 (short) sequence. The N-terminal domain, that lacks any similarity with known domains, is less well conserved (48% similarity) than the putative nucleic acid binding WGR domain (77% similarity) and the PARP catalytic domain (76% similarity). The catalytic core H-Y-E amino acid triad, critical for NAD^+ binding and PARP activity, is conserved (Fig. 2.1) (Kleine and al., 2008). Because the catalytic domain and the core catalytic H-Y-E amino acid triad are conserved, it makes possible the analysis of its biological function using zebrafish as a model.

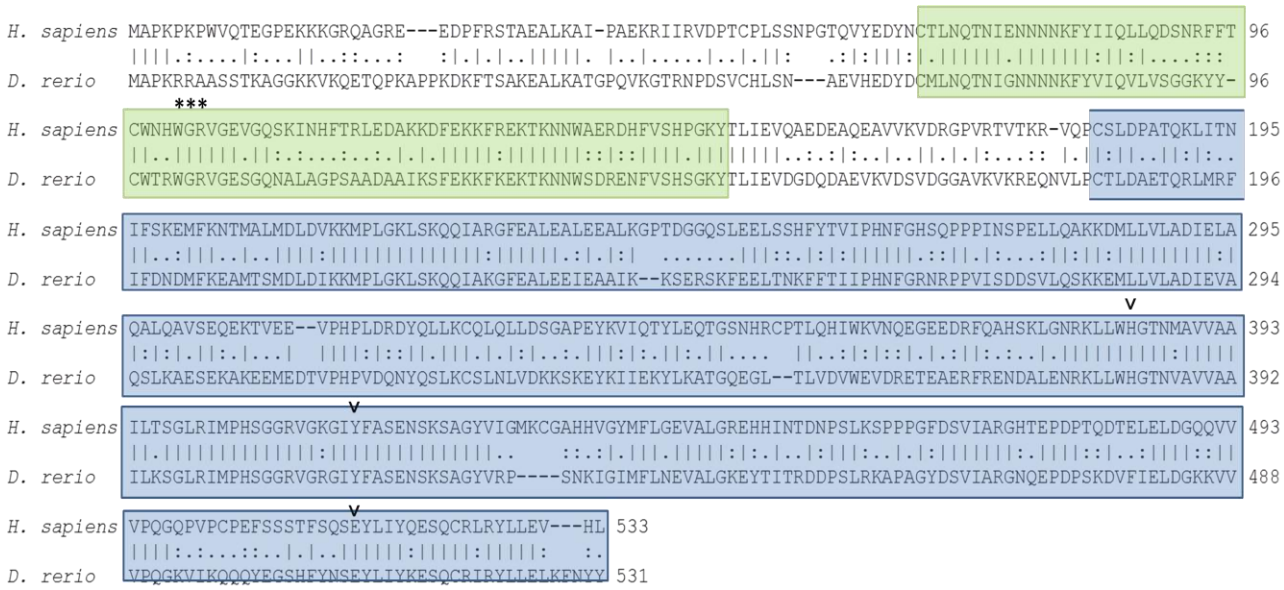

Figure 2.1 Comparison of the amino acid sequences of the human PARP3 (accession number NP_005476) and zebrafish Parp3 (accession number NP_956795). The sequence in the WGR domain (green box) and the catalytic domain (blue box) is well conserved, including the WGR triad (asterisks) and the residues critical for the poly(ADP-ribosyl)ation reaction H-Y-E (>). This figure was produced by the author of the thesis.

3.2 Parp3 is essential for zebrafish development

To address the biological functions of Parp3 during zebrafish development, the function of *parp3* was knocked down by microinjection of anti-sense morpholino oligonucleotides (MOs) into one-cell stage zebrafish embryos. Two non-overlapping MOs, one targeting the transcriptional start site of the parp3 gene (MO1) and the other the 5'UTR sequence immediately upstream of the transcriptional start site (MO2), were used to monitor the effects of reduced Parp3 levels on zebrafish development. Both MOs induced an effective knock-down of Parp3 protein expression (data shown for MO1, Fig. 2.2A) that resulted in important developmental defects and lethality by 5–6 days following fertilization (data shown for MO1 in Fig. 2.2B–D). Antibodies raised against human PARP3 recognize zebrafish Parp3 (Fig. 2.2A). These observations support the notion that zebrafish Parp3 is highly related to human PARP3 at the amino acid level and that PARP3 is an evolutionarily conserved protein in multicellular organisms. Visual inspection of the zebrafish embryos revealed a motility defect 24 hours post-fertilization (hpf) that remained until death of embryos. While wild type embryos and those injected with a control MO present a typical spontaneous contractile movement, embryos injected with parp3 MOs display little movement. By 48 hpf, most *parp3* morphants have not hatched, lack inner ears and pectoral fin buds (Fig. 2.2B), and their pigmentation is drastically delayed (Fig. 2.2C, D). They show a highly curved trunk with very short tail (Fig. 2.2D). The trunk musculature of *parp3* morphants appears normal but the tail bud is ill-developed (Fig. 2.2C). The median fin fold of *parp3* morphants is severely affected (Fig. 2.2C). The symmetrical median fin fold of wild type embryos contrasts with that of morphants which is less developed and particularly perturbed on the dorsal side (Fig. 2.2C, arrow). The fin fold of morphants displays a granular aspect and the actinotrichia (unmineralized structural fibrils of the median fin fold) appear shorter or less

clearly visible. Furthermore, the severity of the phenotype increases with the dose of injected parp3 MO (Fig. 2.2D) and defects are not restored at later times post-fertilization, indicating that they are irreversible consequences of reduced Parp3 expression. Coinjection of a *p53* MO with *parp3* MO1 or MO2 did not rescue most of the observed developmental defects, the exception being the inner ear (Fig. 2.2E). This result indicates that the inner ear is Parp3 and p53-dependant while the other phenotypes are Parp3 dependant only (Robu et al., 2007). Finally, we have tried to rescue the phenotypes of *parp3* morphants by microinjection of newly synthesized RNA from a construct where hPARP3 were put in frame with FLAG. The positive control shows a 65kDa band corresponding to hPARP3-FLAG (Fig.2.2F lane 1). However we did not detect a significantly stronger signal in zebrafish microinjected with the corresponding RNA (Fig.2.2F lane 3) than in wt (Fig.2.2F lane 2). This result indicates that we did not rescue the expression of Parp3 in zebrafish embryo. Nonetheless, developmental defects of Parp3 knockdown are observed with the MO1 and MO2 whereas no such defects were found with the microinjection of a non-targeting MO, which indicates that these phenotypes are specific for Parp3 depletion. Together, the results indicate that a reduced expression of Parp3 has pleiotrophic effects on development and suggest an important function for this protein during development.

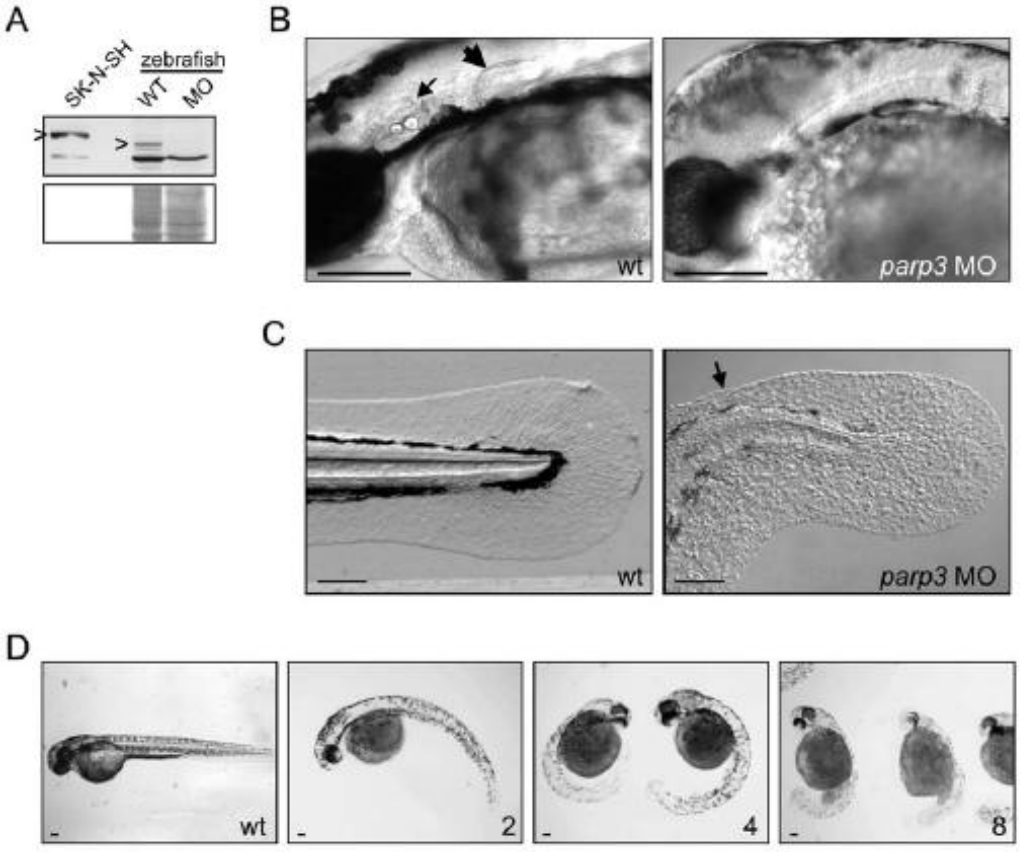
A
SK-N-SH
zebrafish
WT
MO
B
wt
parp3 MO
C
wt
parp3 MO
D
wt
2
4
8

E

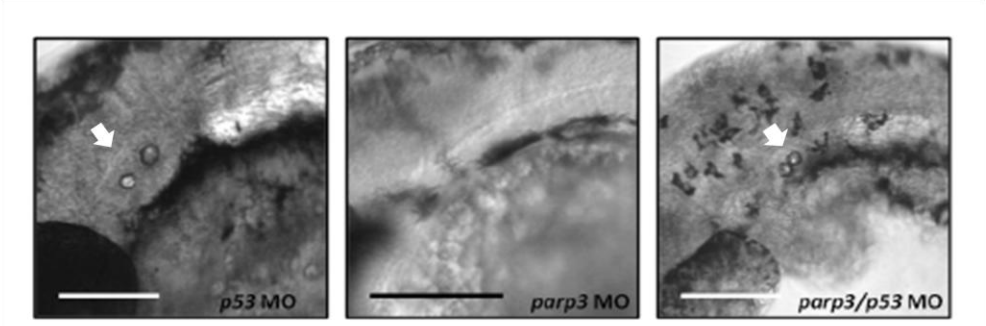
p53 MO
parp3 MO
parp3/p53 MO

F

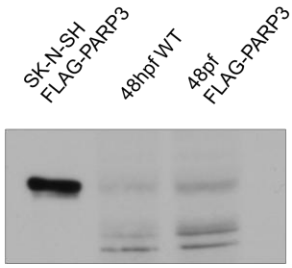
SK-N-SH
FLAG-PARP3
48hpf WT
48pf
FLAG-PARP3

Figure 2.2 Developmental perturbations in zebrafish embryos with impaired *parp3* expression. A. Immunoblot analysis (upper panel) of zebrafish Parp3 in wild type (WT) and *parp3* morphants (MO) using an antibody raised against human PARP3. A whole cell extract of human SK-N-SH cells is shown as a control. The protein bands corresponding to PARP3 are indicated by ‘‘>’’. The faster migrating band corresponds to a non-related protein that cross-reacts with the antibody. The Western blot membrane was stained with Ponceau S as a protein loading control (lower panel). B. Enlarged lateral views of the head regions of 48hpf wild type and *parp3* morphants injected with 4 ng MO1. The inner ears (small arrow) and the pectoral fins (large arrow) in the wt embryos are not formed in the *parp3* morphants. C. Enlarged lateral views of the tail of wild type and *parp3* morphants injected with 4 ng MO1. The median fin fold (arrow) is less developed in the morphants and has a more granular aspect. Effects are more pronounced on the dorsal side (arrow). D. Zebrafish embryos 48hpf injected with increasing amounts of the *parp3*-specific morpholino oligonucleotide MO1 at the one-cell stage (ng amounts indicated in the lower right corner). The short length of morphant embryos, their curved tail and their reduced pigmentation is increasingly severe with increasing amounts of injected MO1. E. Enlarged lateral views of the ear region of 48hpf embryos microinjected with *p53*MO/*parp3*MO. White arrows show the inner ears. F. Immunoblot analysis of zebrafish FLAG-PARP3 in 48hpf wild type (WT) and *parp3* morphants (MO) microinjected with FLAG-PARP3 RNA using a FLAG antibody. A whole cell extract of human SK-N-SH cells is shown as a control. The protein bands corresponding to FLAG-PARP3 are indicated by ‘‘*’’. Lateral views with anterior to the right and dorsal to the top. Scale bars represent 100 µm. Panel A to D

are from Rouleau et al., 2011. Panel B, C and E were produced by the author of the thesis as well as production of the samples for panel F.

3.3 Exploration of the reduced motility in *parp3* morphants

In an effort to further characterize the defects induced by the reduced expression of Parp3, we used transgenic Tg(fli1:EGFP)y1 zebrafish embryos to evaluate the development of the vasculature in *parp3* morphants (Lawson and Weinstein, 2002). Despite the severely distorted aspect of the morphants and their ill-developed tail region, the knock-down of Parp3 does not impair vascular development (Fig. 2.3A). Similarly, developments of the floor plate (Fig. 2.3B) and of motoneurons (Fig. 2.3C) are not altered by the reduced expression of Parp3, therefore an unlikely explanation for the impaired motility of *parp3* morphants.

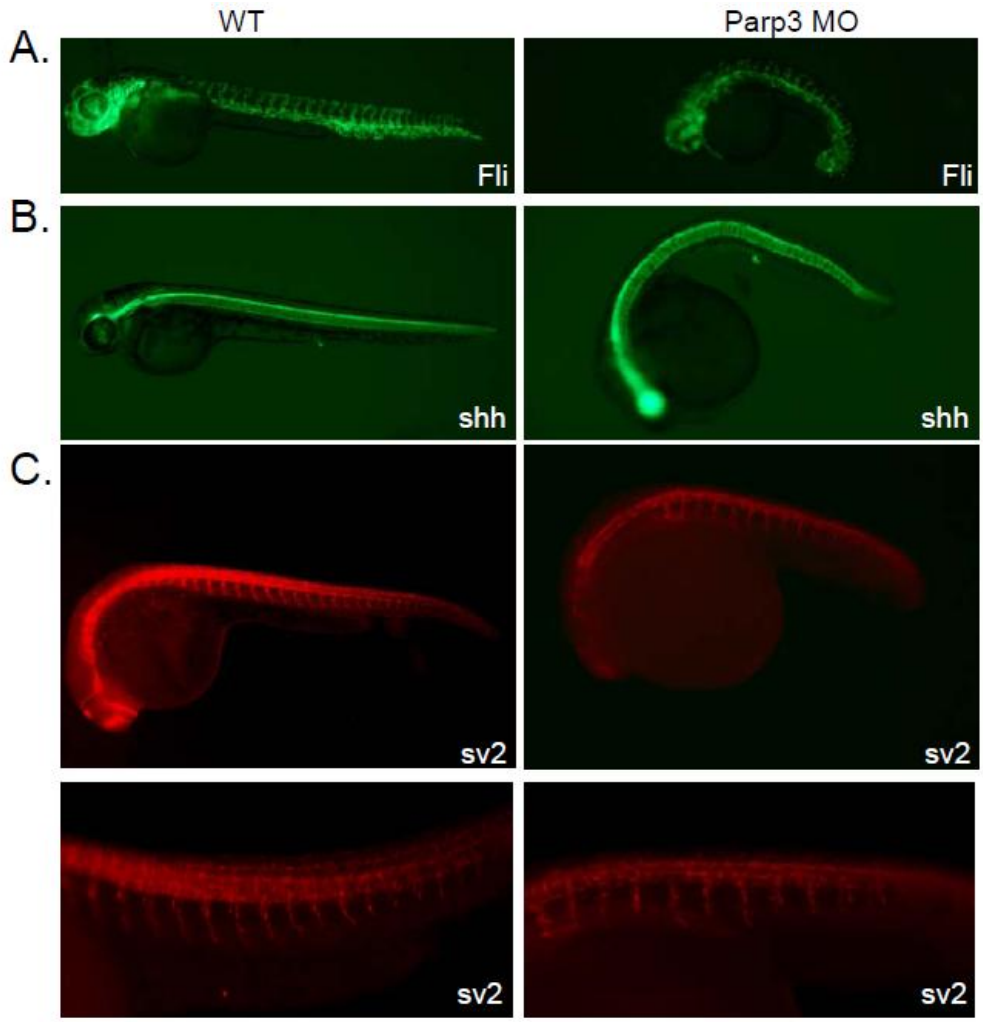

Figure 2.3 Analysis of developmental defects in *parp3* morphants. A. Vasculature development in *parp3* morphants. Tg(fli1:EGFP)^{y1} zebrafish embryos were injected with *parp3* MO1. GFP is expressed exclusively in the vasculature. Vasculature development in *parp3* morphants is similar to that in control embryos, shown here at 48 hpf. B. Neural floor plate development in *parp3* morphants. One-cell embryos from transgenic zebrafish expressing GFP under the control of the sonic hedgehog (*shh*) promoter were injected with *parp3* MO1. GFP is expressed specifically in the floor plate. Despite the highly curved trunk in *parp3* morphants, the neural floor plate pattern is similar to that of control embryos, shown at 48 hpf. C. Motoneuron

development in *parp3* morphants. The distribution of synaptic vesicle 2 (sv2), a marker of motoneurons, was monitored to determine if ill-developed motoneurons could explain the impaired motility of morphants. Wild type zebrafish embryos injected or not with *parp3* MO1 were fixed at 24 hpf and immunostained with an anti-sv2 antibody. Lower images represent higher magnification views of the trunk region. Motoneurons appear to develop normally in *parp3* morphants. Embryos were visualized under a fluorescence microscope. Scale bars represent 100 µm. Figure published in Rouleau et al., 2011. Panel C was produced by the author of the thesis.

3.4 Parp3 regulates sensory placodes development in zebrafish embryos

The identification of several PARP3 targets involved in development led us to assess whether they would be misregulated in zebrafish *parp3* morphants. Among genes potentially regulated by PARP3 in SK-N-SH cells, *SOX9*, *DLX3* and *DLX4* are of particular interest. During development of vertebrate embryos, these transcription factors are crucial in inducing early differentiation programs of neural crest progenitor cells into sensory placodes, oligodendrocytes, sensory neurons of the peripheral nervous system and pigment cells. In zebrafish embryos, orthologs of these genes (*sox9a* and *sox9b*, *dlx3b* and *dlx4b*) encode transcription factors crucial for the specification of non-neural ectoderm and neural crest cells into otic and olfactory placodes, pigment cells and the median fin fold (Akimenko and al., 1994; Solomon and al., 2002; Yan and al., 2005). An altered expression of these genes could therefore result in defective neural crest cell specification and migration. By ISH, we find that the expression of the neural crest specifier *sox9a* is indeed reduced in *parp3* morphants at 10, 16 and 24 hpf (Fig. 2.4 A–F). The high level of expression of *sox9a* in the otic placode (Fig. 2.4A) and later in the otic vesicle (Fig. 2.4B) of wild type embryos is drastically reduced in *parp3* morphants (Fig. 2.4D, E). At 16 hpf, the expression of *sox9a* in the morphant paraxial cells is more diffuse suggesting that the somitogenesis is possibly disturbed (Fig. 2.4B, E). At 24 hpf, *sox9a* is normally expressed in the trunk and in three major areas of the head: the forebrain, the midbrain-hindbrain boundary and the pharyngeal arches (Fig. 2.4C). Expression in these three major sites is lost in the morphants and there is barely any expression in the trunk (Fig. 2.4F). The distal-less related genes *dlx3b* and *dlx4b* encode homeobox transcription factors separated by a common short intergenic region that show largely overlapping expression patterns (Akimenko and al., 1994; Solomon and al., 2002; Esterberg and Fritz, 2009). They are among the earliest transcription factors expressed in the otic

and olfactory placodes, as well as in the median fin fold, a structure that is also affected in *parp3* morphants (Fig. 2.2C). Expression of *dlx3b* at the neural plate border is not severely affected in morphants at 10 hpf (Fig. 2.4 G, J). However, *dlx3b* expression is almost completely lost in the otic vesicles of morphants at 16 hpf (Fig. 2.4 H, K, arrowhead) and 24 hpf (Fig. 2.4I, L). At the same stage, there is also a decrease in *dlx3b* expression in the branchial arches (Fig. 2.4I, L, arrowhead). A reduced expression of *dlx3b* is also apparent in the olfactory placodes at 16 and 24 hpf (Fig. 2.4H, I, K, L). Finally, *dlx3b* expression in the median fin fold of 24h embryos (Fig. 2.4I, arrows) is nearly absent in the *parp3* morphants (Fig. 2.4L). Similar patterns of expression are observed with the *dlx4b* probe (Fig. 2.4M–R). The *neurod* and *nkx2.1a* genes are additional targets predicted from the genomic analysis of PARP3 distribution. The *neurod* gene encodes a bHLH transcription factor and is one of the earliest genes expressed in cranial placodes (Andermann et al., 2002). It plays a determinant role in the formation of the sensory placodes and the peripheral ganglia. The expression of *neurod* appears to be slightly reduced if at all in the trigeminal placode and in the anterior and posterior lateral line placode areas of 16 hpf *parp3* morphant embryos (Fig. 2.5A, B). However, by 24 hpf the overall expression of *neurod* is lower in the morphants than in wild type embryos. The most drastic reductions are seen in the telencephalon, in the octavel/statoacoustic placode, and in the posterior lateral line placode (Fig. 2.5B, D, E–F). In zebrafish, expression of the *NKX2.1* ortholog, *nkx2.1a*, is restricted to the ventral diencephalon (hypothalamus) of early embryos (Rohr and al., 2002), while it is required for the proper development of the thyroid from the pharyngeal endoderm at later stages (Elsalini et al., 2003). While the ChIP-chip analysis revealed that *NKX2.1* is a target of PARP3, expression of *nkx2.1a* does not seem to be markedly affected during the first day of zebrafish development. The expression of *nkx2.1a*, which is mainly confined to the hypothalamus at 16–

24hpf, is similar in wt and *parp3* morphant embryos (Fig. 2.5G–J). Collectively, these observations clearly indicate that reduced Parp3 levels in zebrafish embryos impedes their development through an impaired expression of several transcriptional factors important for the specification of neural crest and sensory placode precursor cells.

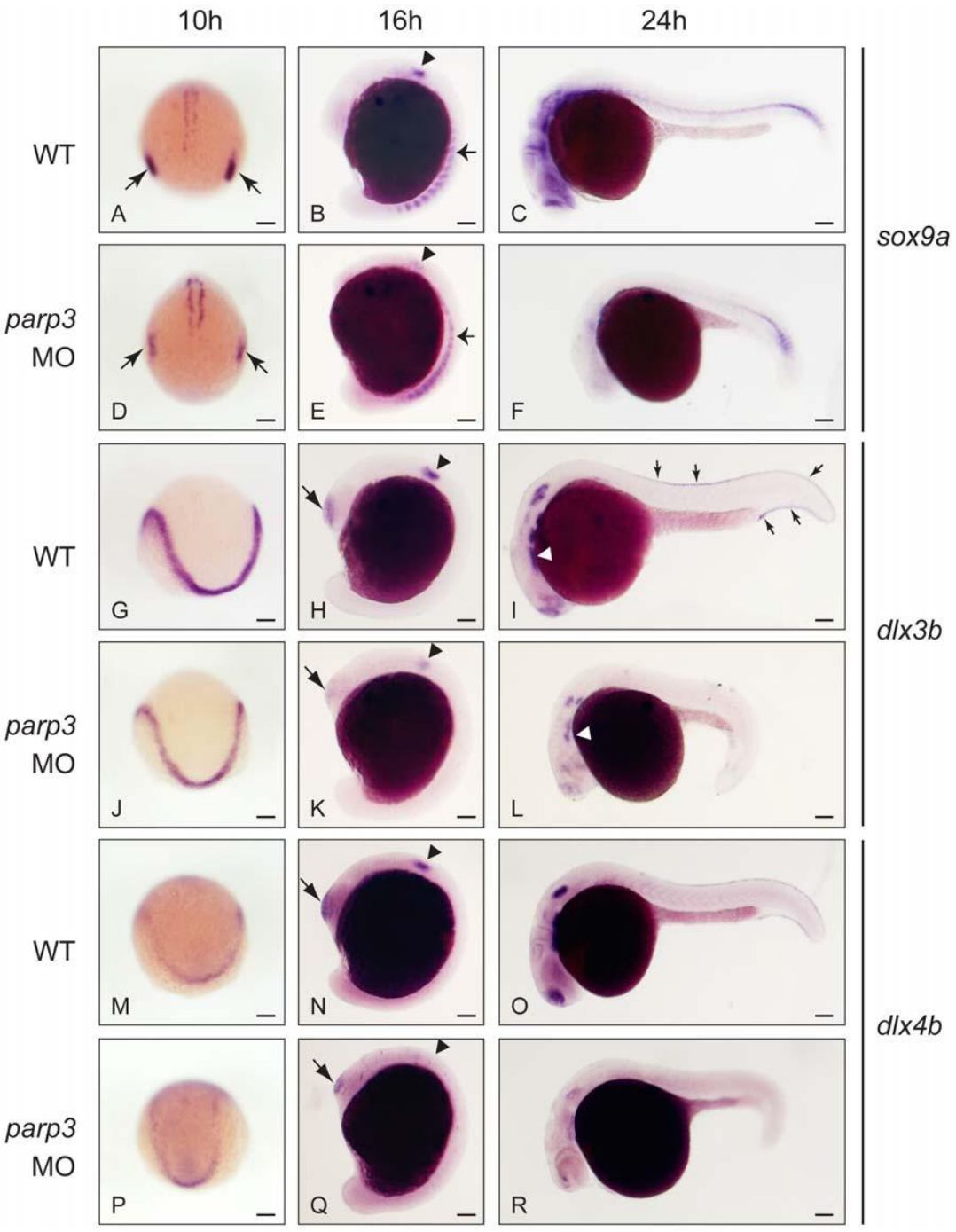

Figure 2.4 Impaired expressions of *sox9a*, *dlx3b* and *dlx4b* in *parp3* morphants. Zebrafish embryos were untreated (WT) or were injected with 4 ng parp3 MO1. Gene expression was detected by in situ hybridization. A–F. The expression of *sox9a* is drastically reduced in the otic

placodes (small arrows) at 10 hpf and in the otic vesicles (arrowheads) at 16 hpf. Expression of *sox9a* in somite cells (small arrows in B and E) appears diffuse in *parp3* morphants. Expression of *sox9a* is almost completely abolished in the head region at 24 hpf (C, F). Expressions of *dlx3b* (G–L) and *dlx4b* (M–R) are minimally affected by *parp3* MO in ectodermal cells at 10 hpf (G, J, M, P) but are significantly reduced in the otic vesicles (arrowheads), olfactory placodes (large arrows) and branchial arches (white arrows) of *parp3* morphants at 16 hpf (H, K, N, Q) and 24 hpf (I, L, O, R). The expression of *dlx3b* and *dlx4b* is abolished in the median fin fold of 24 hpf *parp3* morphant embryos (small arrows in I). Dorsal views of embryos with anterior to the bottom in A, D, G, J, M, P and lateral views with anterior to the left, dorsal to the top, in B, C, E, F, H, I, K, L, N, O, Q and R. Scale bars represent 100 µm. This figure was produced by Vishal Saxena and the results was analysed by the author of the thesis (Rouleau et al., 2011).

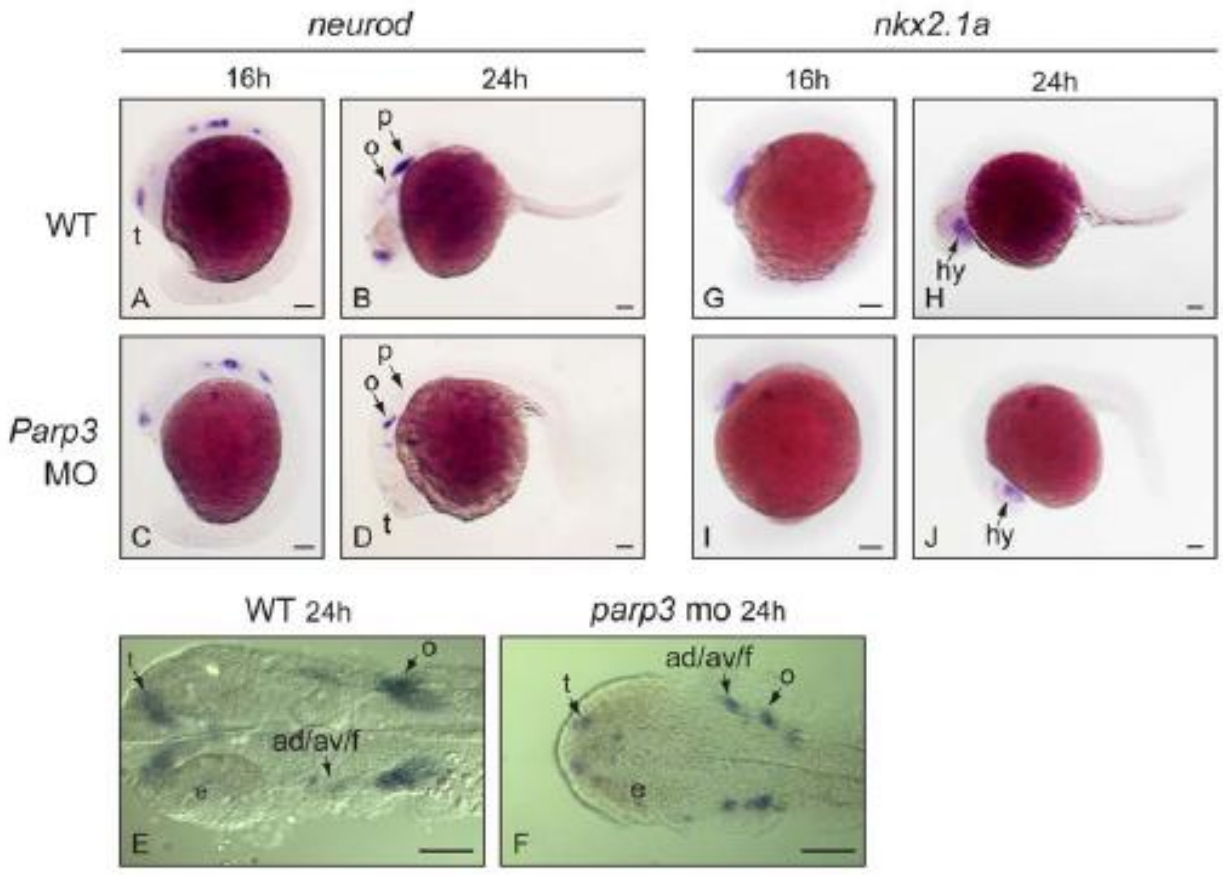

Figure 2.5 Expression of *neurod* and *nkx2.1a* in *parp3* morphants. Expression of: A–F, *neurod* and G–J, *nkx2.1a* were determined in uninjected embryos or in embryos that received 4 ng of parp3 MO1, by in situ hybridization. A–D and G–J are lateral views with anterior to the left, dorsal to the top. E–F are dorsal views of flat-mounted embryos with anterior to the left. ad/av/f: anterodorsal/anteroventral lateral line/facial placodes/ganglia; p:posterior lateral line placode; e: eye; o: octavel/statoacoustic ganglia precursors; t: telencephalon. Scale bars represent 100 µm. Produced by the author of the thesis (Rouleau et al., 2011).

3.5 Parp3 is an important regulator of neural crest cell specification

Since we have identified different patterns of expression of neural crest specifiers we examined the formation and migration of neural crest cells in *parp3* morphants by monitoring the expression of the neural crest cell marker crestin (Luo and al., 2001) by whole mount in situ hybridization (ISH) in wild type and *parp3* morphant zebrafish embryos. We find that the expression of crestin is indeed altered in *parp3* morphants (Fig. 2.6). At 16 hpf, crestin is normally expressed in premigratory neural crest cells and in neural crest cells migrating from the most anterior trunk segments (Luo and al., 2001) (Fig. 2.6A). In *parp3* morphants however, the expression of crestin is generally reduced with most of the remaining expression limited to anterior trunk segments (Fig. 2.6B). Crestin expression is nearly undetectable in the hindbrain region. At 24 hpf, crestin expression could not be detected in the head and tail regions, while the expression in the trunk of 24hpf-*parp3* morphants appears to be reduced (Fig. 2.6C, D). As crestin was shown to be expressed in all neural crest cells (Luo and al., 2001), our observations suggest a general perturbation in neural crest cell development in embryos with reduced Parp3 expression.

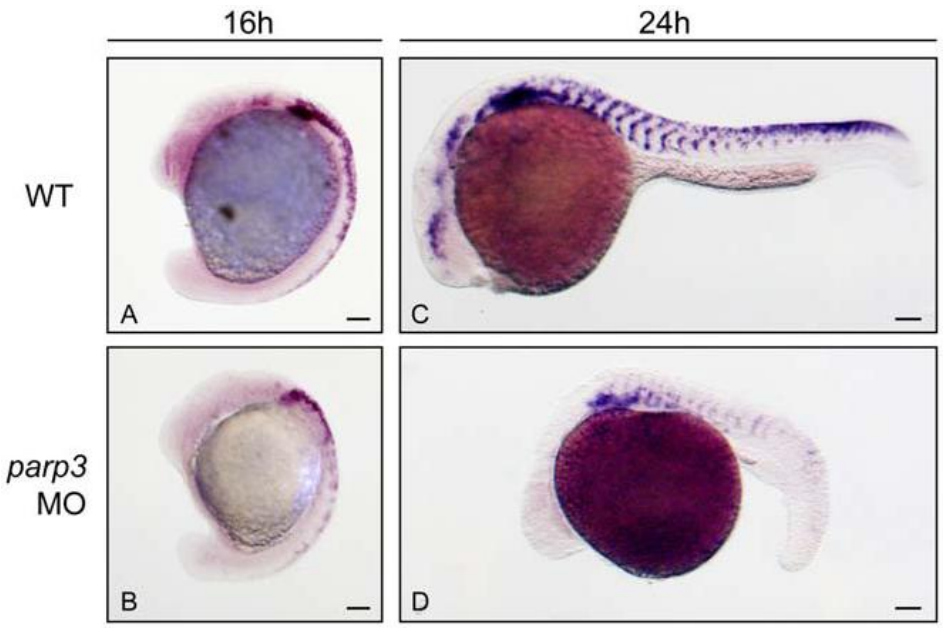

Figure 2.6 Expression of the neural crest cell marker *crestin* is impaired in *parp3* morphants. Zebrafish embryos were untreated (WT) or injected with 4 ng *parp3* MO1 and *crestin* expression was monitored by in situ hybridization. A. In 16 hpf WT embryos, crestin is expressed in premigratory neural crest cells and in neural crest cells migrating in the anterior trunk segments. B. In 16 hpf *parp3* morphants, *crestin* expression appears to be generally reduced. C. By 24 hpf, *crestin*-positive cells are distributed along the anterior-posterior axis, in neural crest migratory pathways of WT embryos. D. In 24 hpf *parp3* morphants, *crestin* expression is no longer detectable in the head and is markedly reduced in the trunk. Lateral views of embryos are shown with anterior to the left and dorsal to the top. Scale bars represent 100 µm. This figure was produced by the author of the thesis (Rouleau et al., 2011).

3.6 Parp3 depletion leads to an overall increase of programmed cell death

Because of the prominent role played by poly(ADP-ribosyl)ation in DNA damage response (DDR), and my previous results showed that Parp3 is an important neural plate border specifier (thereby influencing neural crest development), we hypothesized that the decrease in Parp3, within neural crest cells of the zebrafish, would lead them to undergo apoptosis because of the putative deficiency to repair the DNA into these cells. Acridine orange is a vital dye commonly used to assess the number of cells undergoing apoptosis (Tucker and Lardelli, 2007; Walters et al., 2009; Shu et al. 2010). Apoptotic cells are stained by acridine orange and appear as small foci. Consequently, I performed an apoptosis assay to verify this assumption. Three independents essays were conducted on *parp3* morphant and wt embryos using approximately 30 embryos each at 24hpf stage (Fig. 2.7). Zebrafish depleted in Parp3 show a massive increase in cells undergoing apoptosis as compared to wt. However, this method did not permit the identification of specific cells or location enriched in cells undergoing programmed cell death in the *parp3* morphants. The enlarged views of the head and trunk as well as the tail rather demonstrate a general increase in apoptosis. Although we did not perform a quantitative analysis, it is visually evident that there is an overall increase in apoptosis in zebrafish reduced in Parp3 expression.

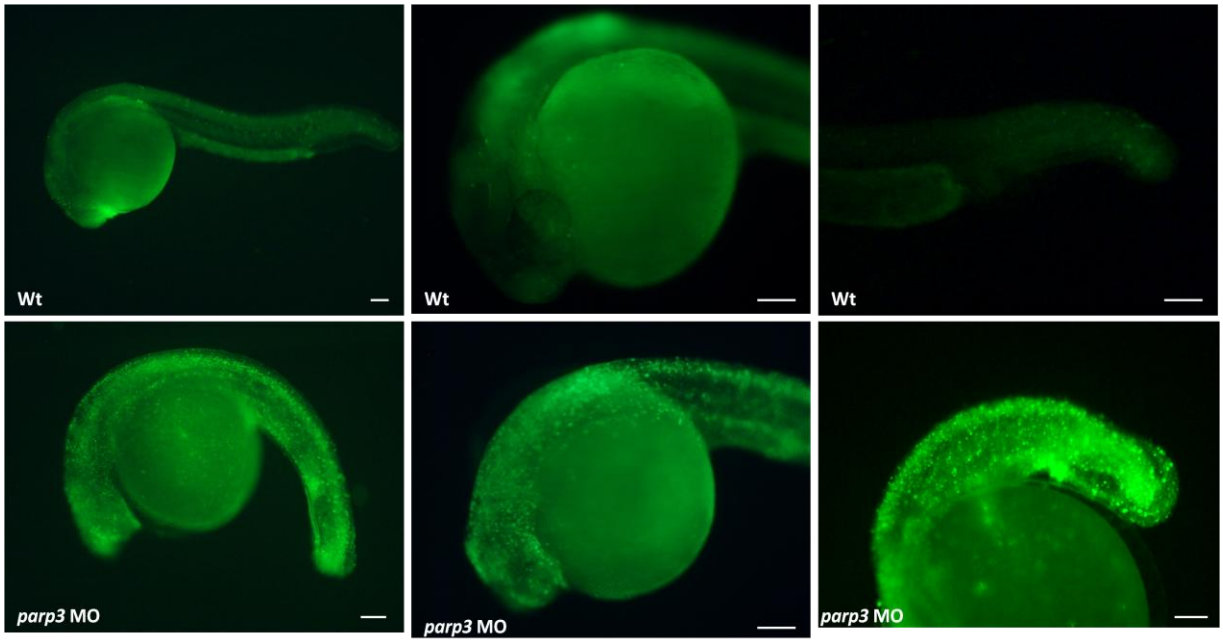

Figure 2.7 Embryos with reduced Parp3 expression undergo an overall increase of programmed cell death. 24hpf wt (upper panel) and *parp3* morphants (lower panel) were stained with acridine orange. Whole embryos are shown on the left. Enlarged views of the anterior part and posterior part of the body are shown in the center and on right, respectively. Embryos were visualized under UV light and a green fluorescent filter with excitation 470/40. Dead or dying cells appear as small foci. Scale bars represent 100 µm. Produced by the author of the thesis.

3.7 Actinotrichias are lost close to the median line of the median fin fold

To better characterize the underdeveloped median fin fold of *parp3* morphants, I have first stained 48hpf *parp3* morphants and wild type zebrafish with a Sirius red solution saturated in picric acid to look at collagens of the actinotrichias (Fig. 2.8A) (Santamaría and Becerra, 1991; Santamaría and al., 1992).We observe a perturbation of the collagen structure in *parp3* morphant; the typical collagen rays are lost and present a disorganized arrangement of collagen molecules (Fig.2.8A). Because collagens are very important constituents of the actinotrichia (Durán et al., 2011) this result can explain why the actinotrichias are so much affected in *parp3* morphants. Furthermore it has been demonstrated that actinotrichias are essential for the proper migration of the mesenchymal cells from the distal tip of the tail to the distal end of the fin folds (Wood and Thorogood, 1984; Zhang et al., 2011). Thus we have used the transgenic line Enhancer trap 37 (ET37) to look at the migration of these cells in *parp3* morphants because these fish express the green fluorescent protein (GFP) in mesenchymal cells within the fins throughout development. As expected, there is a lack of actinotrichia in the median fin fold of *parp3* morphants. It seems that the deficiency is concentrated around the median line of the median fin fold (Fig 2.8B) because the migration of mesenchymal cells is disorganized and cells seem to migrate randomly through the fin whereas on the side of the fins they are following the path of the actinotrichias. Moreover we can observe folding of the fin caused by the lack of support structure, the actinotrichias. Collectively, these results indicate that actinotrichias are affected in zebrafish reduced in Parp3 expression.

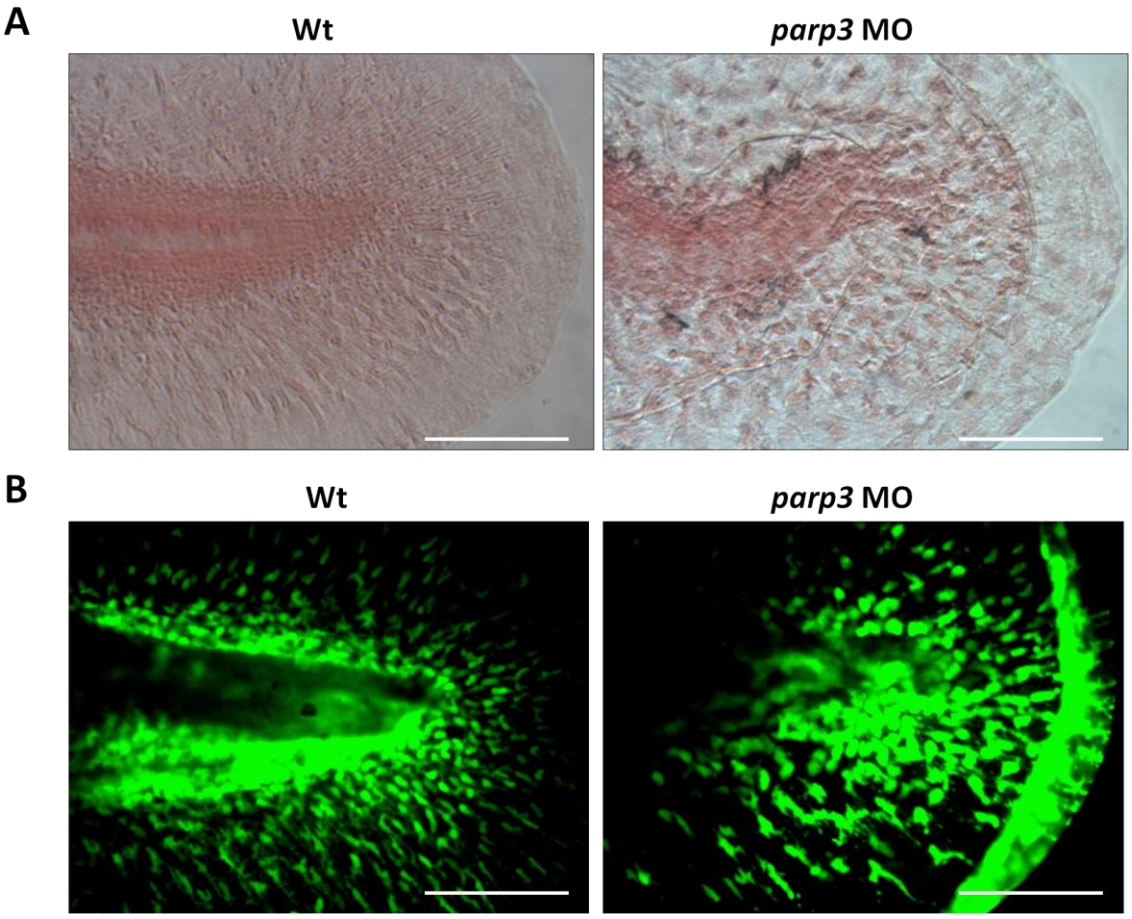

Figure 2.8 Actinotrichia deficiencies in zebrafish with impaired Parp3 function. A. Enlarged lateral views of the tip of the median fin fold of 48hpf *parp3* morphants and Wt larvae stained with 0.1% Sirius red in a saturated picric acid solution. B. Enlarged lateral views of the tip of the median fin fold of 48hpf transgenic larvae, Enhancer trap 37 (ET 37) microinjected with 4ng parp3 MO1 or uninjected controls. Lateral views with anterior to the right and dorsal to the top. Scale bars represent 500 µm. Produced by the author of the thesis.

3.8 Zebrafish PARP1 and PARP2

As mentioned in the introduction, the human PARP1 and PARP2 proteins are also conserved in zebrafish. Because we identified a function in development for zebrafish Parp3, we aimed to explore the role of zebrafish Parp1 and Parp2 as well. We first aligned the amino acid sequences of PARP1 and PARP2 with their corresponding zebrafish orthologues (Fig.2.9). Zebrafish Parp1 comprises 1013 amino acids and shares 84 % sequence similarity with hPARP1indicating that it is well conserved. Although the BRCT domain of Parp1 is not well conserved, its other domains are well conserved: the two zinc finger domains share 85 and 87% sequence similarity, the WGR domain share 85% sequence similarity and the catalytic domain comprises 92% sequence similarity with hPARP1 (Fig. 2.9A). The catalytic core H-Y-E amino acid triad, critical for NAD^+ binding and PARP activity, is conserved (Fig.2.9A). Zebrafish Parp2 comprises 648 amino acids and is less well conserved than Parp1, with 69% similarity with the human sequence. The WGR (85% similarity) and the catalytic domains (83% similarity) of Parp2 are very well conserved as well as the catalytic core H-Y-E amino acid triad (Fig.2.9B). However, the putative basic DBD of hPARP2 is not conserved in the zebrafish sequence. Surprisingly, it appears that the zebrafish Parp2 possesses a WWE domain, located close to the N-terminal of the protein. The WWE domain is a recently characterized pADPr binding module. In humans, it is found in other PARPs (Schreiber and al., 2006) as well as in a subfamily of E3 ubiquitin ligases such as RNF146, important for the regulation of protein stability (Wang et al., 2012). Taken together, these observations suggest that the function of zebrafish PARP2 could differ from those of its human orthologue.

A


H. sapiens MAESSD-KLYRVEYAKSGRASCKKCSESIPKDSLRMAIMVQSPMFDGKVPHWYHFSCFWKVGHSIRHPDVEVDGFSELRWDDQQKVKKTAEAGGVTG-KG 98
D. rerio MADSQDDKLYKAEYAKSGRASCKKCKDNIAKDSLRMAIMVQSPMFDGKVPHWHHFSCFW-LRAAVQSPS-DISGFTDLRWDDQEKVKTAIESGGATGGKG 98
H. sapiens QDGIGSKAEKTLGDFAAEYAKSNRSTCKGCMEKIEKGQVRLSKKMVDPEKPQLGMIDRWYHPGCFVKNREELGFRPEYSASQLKGFSLLATEDKEALKKQ 198
D. rerio GQKGAAKGEKTLNDFAVEYAKSNRSTCKGCDQKIEKDQIRVSKKTVDPEKPQLGLIDRWYHTGCFVSRREELIFKPEYSAAQLKGFAVLRDEDKEELKKR 198
H. sapiens LPGVKSEGKRKGDEVDGVDEVAKKKSKKEKDKDSKLEKALKAQNDLIWNIKDELKKVCSTNDLKELLIFNKQQVPSGESAILDRVADGMVFGALLPCEEC 298
D. rerio LPAVKSEGKRKADEVDG------GVSKKQKKEDEKLEQNLKDQSQLIWGIKDKLKKFCSINDMKELLIANSQEVPSGESNIVDRLSDCMAFGSLKPCETC 292
H. sapiens SGQLVFKSDAYYCTGDVTAWTKCMVKTQTPNRKEWVTPKEFREISYLKKLKVKKQDRIFPPETSASVAATPPPSTASAPAAVNSS------ASADKPLSN 392
D. rerio KGQLVFKSDAYYCTGDISAWTKCVFKTQTPDRKDWVTPKEFSEIPFLKKFKFKRQDRVFPKDAPPAAATPSSGSTTSAATSVSSASKNLTEAPADKPLTG 392
H. sapiens MKILTLGKLSRNKDEVKAMIEKLGGKLTGTANKASLCISTKKEVEKMNKKMEEVKEANIRVVSEDFLQDVSASTKSLQELFLAHILSPWGAEVKAEPVEV 492
D. rerio MKLLAVGKLSKNKDDLKKFVEDLGGKITGTASKAALCISSKKEIEKMSKKMEEVRDAGVRVVADDFLTDIKESGKALQELISLHAISPWGAEVKVE-APA 491
H. sapiens VAPRGKSGAALSKKSKGQVKEEGINKSEKRMKLTLKGGAAVDPDSGLEHSAHVLEKGGKVFSATLGLVDIVKGTNSYYKLQLLEDDKENRYWIFRSWGRV 592
D. rerio AAAATKSTGAHSSKSTGKVKEEEGGSKSKKMKLTVKGGAAVDPDSGLENCAHVLEQNGKIYSATLGLVDIVRGTNSYYKLQLLEDDVQKRYWVFRSWGRV 591
H. sapiens GTVIGSNKLEQMPSKEDAIEHFMKLYEEKTGNAWHSKNFTKYPKKFYPLEIDYGQDEEAVKKLTVNPGTKSKLPKPVQDLIKMIFDVESMKKAMVEYEID 692
D. rerio GTTIGGNKLDKFYDKNSAMDNFCGVYEEKTGNAWASSNFTKYPNKFYPLEIDYGQDEEAVKKLTQSAGAKSQLEKPVQDLIRMIFDVESMKKAMVEFEID 691
H. sapiens LQKMPLGKLSKRQIQAAYSILSEVQQAVSQGSSDSQILDLSNRFYTLIPHDFGMKKPPLLNNADSVQAKVEMLDNLLDIEVAYSLLRGGSDDSSKDPIDV 792
D. rerio LQKMPLGKLSKRQIQSAYSLLSEVQQAVADSSSESLILDLSNRFYTLIPHDFGMKKPPLLSNVDYIQQKVQMLDNLLDIEVAYSLLRGGVENNEKDPIDI 791
H. sapiens NYEKLKTDIKVVDRDSEEAEIIRKYVKNTHATTHNAYDLEVIDIFKIEREGECQRYKPFKQLHNRRLLWHGSRTTNFAGILSQGLRIAPPEAPVTGYMFG 892
D. rerio NYEKLKTKIEVVDKSSHEAQLILQYVKNTHAATHNTYTLDVEEIFKIEREGEYQRYRPFKELPNRQLLWHGSRTTNYAGILSQGLRIAPPEAPVTGYMFG 891
H. sapiens KGIYFADMVSKSANYCHTSQGDPIGLILLGEVALGNMYELKHASHISKLPKGKHSVKGLGKTTPDPSANISLDGVDVPLGTGISSGVNDTSLLYNEYIVY 992
D. rerio KGVYFADMVSKSANYCHTSQADPVGLILLGEVALGNMHELKKASHITKLPKGKHSVKGLGRSAPDPRATVSLNGVDIPLGKGMNTNIDDTSLLYNEYIVY 991
H. sapiens DIAQVNLKYLLKLKFNFKTSLW 1014
D. rerio DVSQVNLKYLLKIRFNYQTSLW 1013

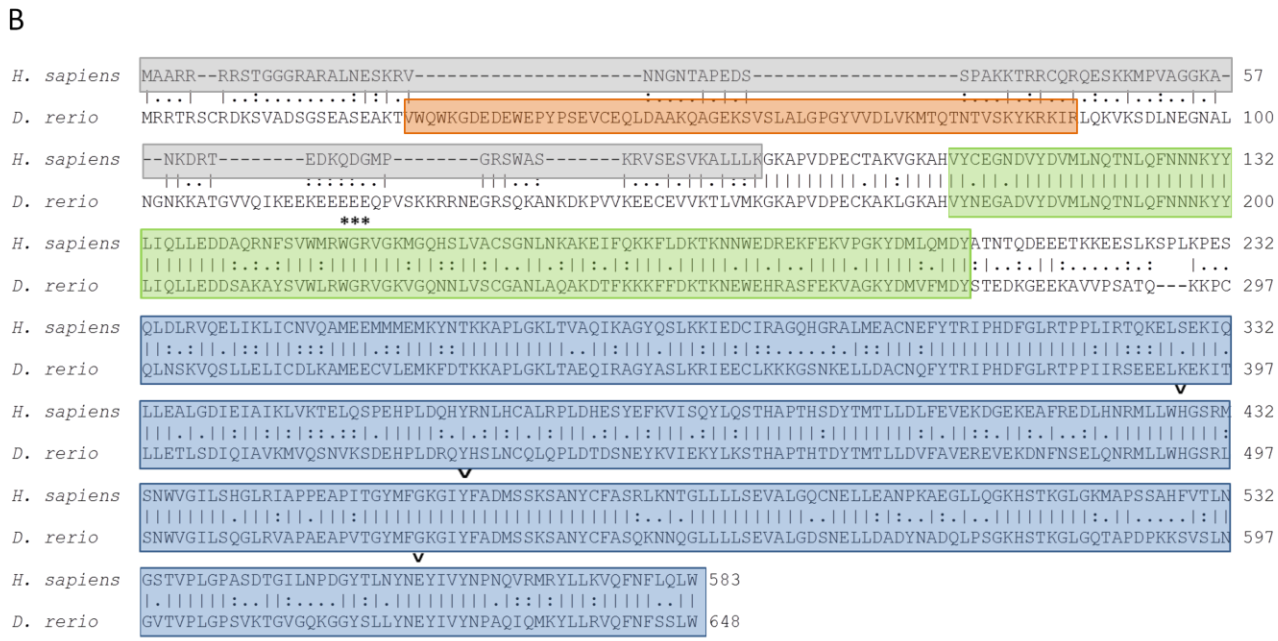

Figure 2.10 Comparison of the amino acid sequences of the human PARP1 and PARP2 with their respective zebrafish orthologs Parp1 and Parp2. A. Comparison of the amino acid sequences of the human PARP1 (NP_001609) with the zebrafish Parp1 (NP_001038407). The sequence in the WGR domain (green box) and the catalytic domain (blue box) is well conserved, including the WGR triad (asterisks) and the residues critical for the poly(ADP-ribosyl)ation reaction H-Y-E (>). The sequences in the 2 zinc finger domains (yellow box) are well conserved as well but not the BRCT domain (pink box). B. Comparison of the amino acid sequences of the human PARP2 (NP_005475) with the zebrafish Parp2 (NP_001191199). The sequence in the WGR domain (green box) and the catalytic domain (blue box) is well conserved, including the WGR triad (asterisks) and the residues critical for the poly(ADP-ribosyl)ation reaction H-Y-E (>). However the DNA binding domain (grey box) is not conserved and the zebrafish Parp2 comprise a WWE domain (orange box) which is not present in the human PARP2. The figure was produced by the author of the thesis.

3.9 Parp3 function differs from that of Parp1 in zebrafish

I have knocked-down Parp1 and Parp2 independently by microinjection of MO specific to each gene into one-cell stage embryos. I have also knocked down both genes by co-injection of *parp1* MO and *parp2* MO since it is known that Parp1 and Parp2 have complementary functions in mammals (Ménissier-de Murcia and al., 2003). It seems that both MOs resulted in protein depletion but knock-down of Parp1 was the most efficient (Fig. 2.10A) based on activity assays. This poly(ADP-ribosyl)ation assay was performed because of the lack of specific antibodies for the two zebrafish proteins. The "activity blot" assay is based on the "Western blot" type transfer of protein extracts on a membrane after which the proteins are renaturated. This is followed by a PARP assay on the blot, consisting in incubating the membrane with activated DNA and NAD^+ in a PARP assay buffer for 1 hour to allow pADPr synthesis (Shah et al., 1995). PARP catalytic activity present in the sample can be indirectly detected by a polyclonal pADPr antibody (96-10). With human cell extracts, this method allows the detection of PARP1 and PARP2 (Fig. 2.11A, lane 6) but not PARP3. The lack of detection of PARP3 activity in this assay is likely due to a poor renaturation (M. Rouleau and G. Poirier, personal communication). We observed various bands on the activity blot (Fig. 2.11A lane 1-5) as compared to the homogenous control SK-N-SH cell line (Fig. 2.11A lane 6). Although we cannot exclude that some of these bands represent pADPr synthesized from other PARPs, most of these are likely the result of PARP1 degradation products. Most of the bands are reduced in intensity in the *parp1* morphant extracts (Fig 2.11A, lanes 2, 3), suggesting that they result from Parp1 activity. Some non-specific cross-reactivity between the anti-pADPr antibody 96-10 and zebrafish proteins may also occur. To better interpret the results, we have measured the intensity of the signals from the activity blot and the loading control (Ponceau S) by densitometry and produced pADPr/proteins ratios where the WT

ratio were fixed to 100% (Fig.2.9A). The global pADPr synthesis is reduced in *parp1* morphants extracts, indicating that Parp1 expression is reduced in these morphants (Fig.2.11A lanes 2 and 3). Of note, Parp1 has about the same molecular weight as hPARP1. We observed a dramatic decrease in the 113 kDa band. Moreover, the pattern of pADPr is different compared to WT and pADPr/proteins ratio show a decrease in activity of about 75% when compared to WT. This indicates that the knock-down of Parp1 was efficient. Parp2, as explained above, is less well conserved in zebrafish (Fig.2.10). Indeed the protein has an additional domain not found in hPARP2, the WWE domain found in other PARPs (Amé et al., 2004), which confers to zebrafish PARP2 a molecular weight of 73kDa, instead of 62 kDa. It is not possible to conclude that the band indeed corresponds to Parp2 based on this result. However the ratio indicates a 29.6 % decrease in activity (Fig2.11A lane 4) and the pattern of pADPr is different from that of *parp1* morphants. This suggests that Parp2 was knocked-down but perhaps only partially. For the double knock-down (Fig.2.11 lane 5), the ratio shows a 67.4 % decrease in activity. Moreover we observed a different pADPr pattern than *parp1* morphants which suggests that not only *parp1* was knocked down. Overall, poly(ADP-ribosyl)ation was decreased in the three knock-down.

Parp1 morphants, *parp2* and *parp1/2* morphants do not exhibit most of the developmental defects of *parp3* morphants. Indeed the inner ear and pectoral fins are formed and appear normal. Also the pigmentation does not decrease in these morphants (Fig. 2.10B). However, most *parp1* morphants display a median fin fold phenotype similar to that of *parp3* morphants (Fig.2.10C): we noticed a granular aspect and the actinotrichias are less clearly visible although the dorsal side is as developed as the ventral side. Morphants appear similar to WT in size but one third of *parp1* morphants are smaller and show the approximate size of *parp3* morphants (inferred from 5

independent experiments). The same third also have a smaller tail that is curved in many orientations (Fig.2.10D). To summarize Parp1 knock-down was effective and morphants do not display most of the *parp3* morphants phenotype. This result argues for a different function for Parp1 and Parp3 in zebrafish. The partial knock-down of Parp2 does not affect the zebrafish embryos. This may suggest that Parp2 is different from Parp3 given the fact that very low amount of *parp3* MO is needed to perturb early development. However, we cannot exclude that the residual Parp2 expression is sufficient to achieve those Parp2 functions.

A

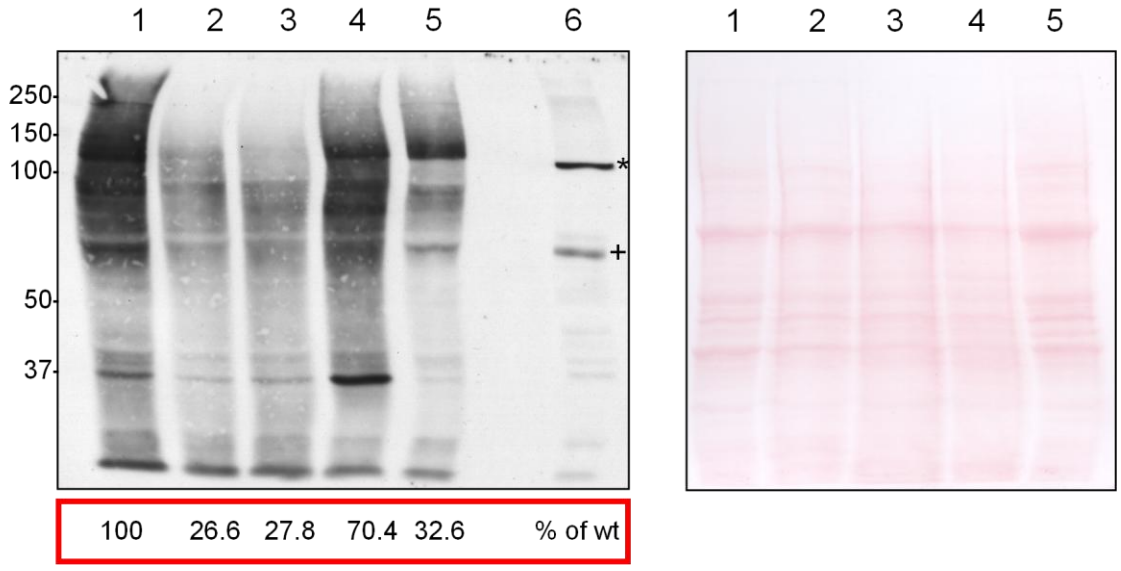

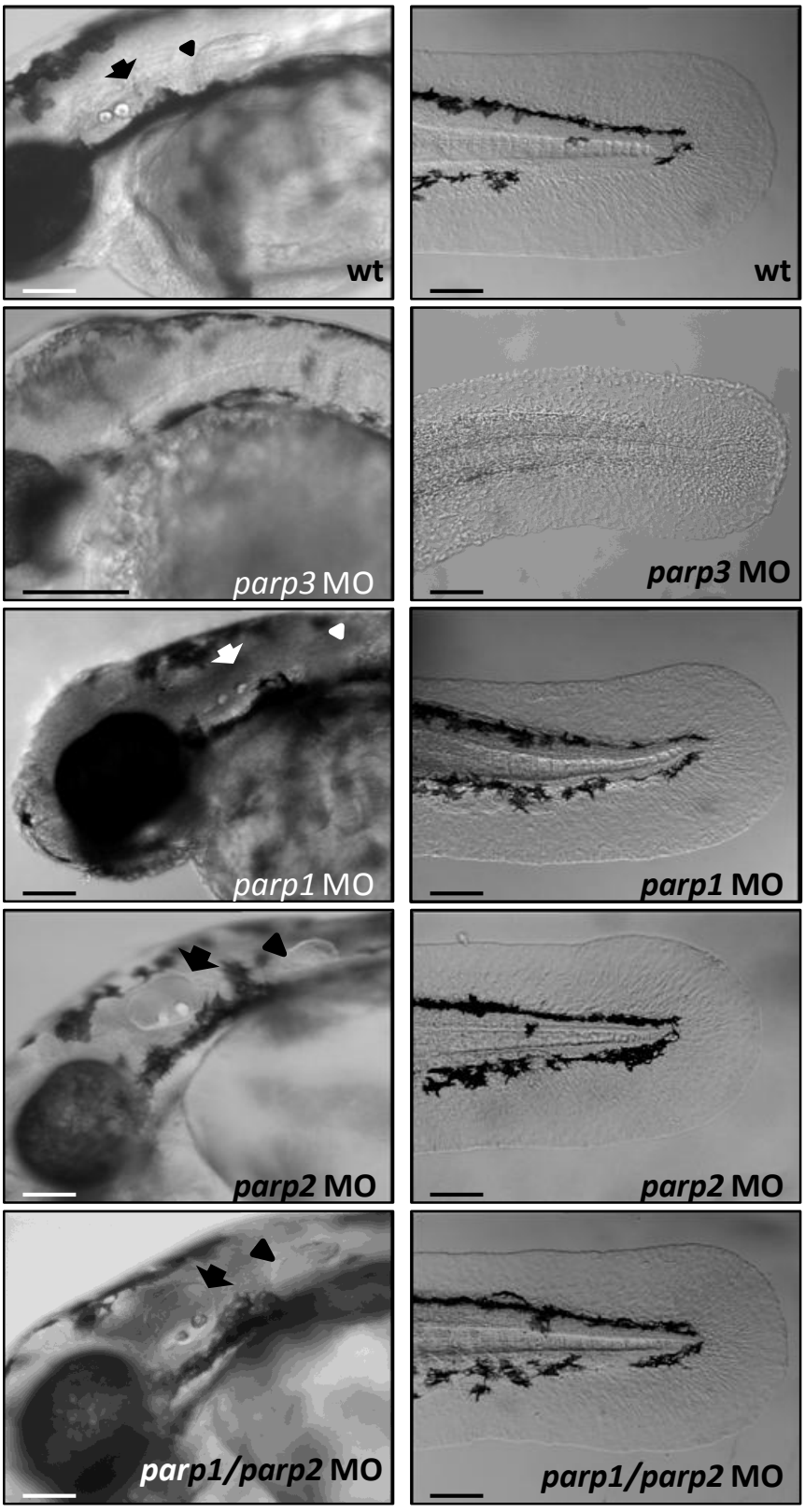
wt
wt
parp3 MO
parp3 MO
parp1 MO
parp1 MO
parp2 MO
parp2 MO
parp1/parp2 MO
parp1/parp2 MO

D

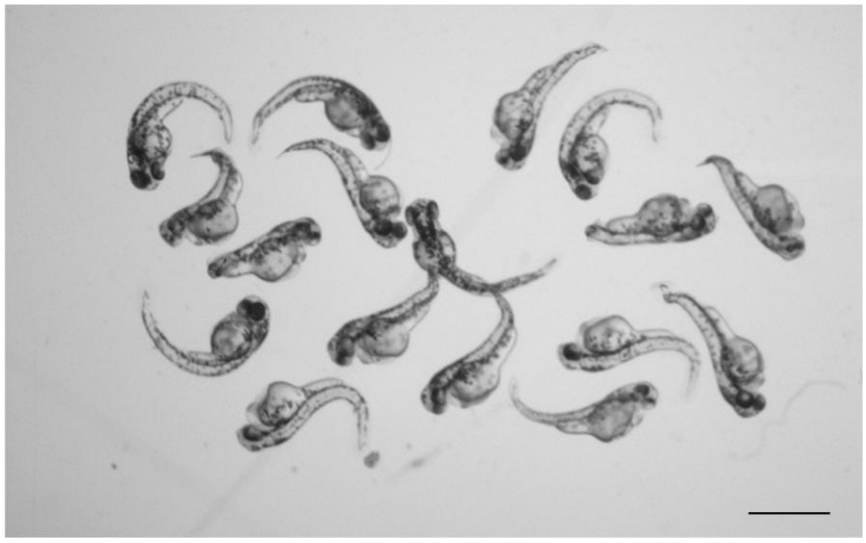

Figure 2.10 Comparison of zebrafish embryos with impaired Parp3 expression and those with impaired Parp1 and/or Parp2 expression. A. Activity blot analysis (left panel) for PARP poly(ADP-ribosyl)ation of zebrafish in WT (lane 1), large *parp1* morphants (lane 2), small *parp1* morphants (lane 3), *parp2* morphants (lane 4) and *parp1/2* morphants (lane 5). A whole cell extract of human SK-N-SH cells is shown as a control (lane 6). The protein band corresponding to PARP1 is indicated by ‘‘*’’ and to PARP2 by ‘‘+’’ in SK-N-SH cells. The blot membrane was stained with Ponceau S as a protein loading control (right panel). Band intensities were measured by densitometry and pADPr/proteins ratios relative to WT are shown in the red box. B. Enlarged lateral views of the head regions of 48hpf wild type, *parp3* morphants injected with 4 ng MO1, *parp1* morphants injected with 6ng MO, *parp2* morphants injected with 6ng MO and *parp1/parp2* injected with 4ng *parp1*MO and 4ng *parp2* MO. Inner ears are shown by black arrows and pectoral fins by black arrowheads C. Enlarged lateral views of the tail of wild type, *parp3* morphants, *parp1* morphants, *parp2* morphants and *parp1/2* morphants, all with same quantity of MO as in panel B. The median fin fold (arrow) is less developed in the *parp3* and *parp1* morphants than in WT. *Parp2* and *parp1/2* morphants show the same aspect as WT. D.

33% of *parp1* morphants at 48hpf show a smaller size and a curved tail. Lateral views with anterior to the right and dorsal to the top. Scale bars for panel B and C represent 100 µm. The scale bar on panel D represents 1000 µm. The poly(ADP-ribose) activity (panel A) was performed by D^{re} Michèle Rouleau while the samples were produced and prepared by the author of the thesis. Panel B and C were produced by the author as well.

4 Discussion

4.1 Developmental transcriptions factors bound by human PARP3 are regulated by its zebrafish orthologues

Preceding this thesis, an analysis of PARP3 genomic occupancy by ChIP-chip in a human cell line determined that chromatin-associated PARP3 corresponds to promoter regions of genes involved in development, especially those involved in neurogenesis (Rouleau et al., 2011). For this reason, we explored the expression of several orthologues of these genes in zebrafish *parp3* morphants by ISH. Surprisingly, I discovered that the expression of all genes surveyed, except *nkx2.1a*, was impaired at early stages of development following the down regulation of *parp3*, thereby indicating that the expression of these genes is Parp3-dependent. However, it is not known whether this is a direct or indirect effect. The expression of *parp3* during zebrafish embryogenesis, which has been partially determined by ISH (Thisse and Thisse, 2004), is consistent with Parp3 exerting regulatory functions at these early stages. By the end of gastrulation (10 hpf), *parp3* is expressed at a basal level throughout the embryo with a stronger expression in the main body axis, whereas during segmentation (10 hpf–16 hpf), *parp3* expression is concentrated in the notochord. By 24 hpf, *parp3* expression is concentrated in the anterior/head region although not restricted to a specific structure. The knock-down of Parp3 revealed embryonic structures with impaired expression *of sox9a, dlx3b/dlx4b* and *neurod* within these regions at corresponding stages. Of note, the pattern of wild type expression of *sox9a* (Yan et al., 2005; Rau et al., 2006), *dlx3b/dlx4b* (Akimenko et al., 1994; Thisse and Thisse, 2004) as well as that of *neurod* (Andermann and al., 2002) determined in this thesis, is consistent with previous observations.

4.2 Parp3 regulates the specification of the neural plate borders

Under the influence of a specific set of transcription factors, multipotent precursor cells of the neural plate borders give rise to the preplacodal ectoderm and to precursors of the neural crest cells. Subsequently, an important gene regulatory network orchestrates the formation, migration and differentiation of neural crest cells into cells of the parasympathetic nervous system, melanocytes, smooth muscle cells and craniofacial cartilage, among others (Sauka-Spengler and Bronner-Fraser, 2008; Haldin and LaBonne, 2010). The SoxE family transcription factors SOX8, SOX9, SOX10 are critical neural crest ‘‘specifiers’’ together with DLX3 and DLX4 (Solomon et al., 2002; Haldin and LaBonne, 2010). We found that *Sox9a* expression and *dlx3b/dlx4b* expression are Parp3-dependent. Therefore, it appears that Parp3 plays a key transcriptional regulatory function in the neural crest of early zebrafish embryos. While the neural crest is forming, the preplacodal ectoderm differentiates into sensory placodes from which are derived all of the cranial sensory ganglia. The SoxE family transcription factors SOX8, SOX9, SOX10 are also critical to direct proper differentiation of the preplacodal ectoderm together with DLX3 and DLX4 (Solomon et al., 2002; Haldin and LaBonne, 2010). In the otic placodes and in the olfactory placodes, expression of *sox9a*, *sox9a* and *dlx3b/dlx4b*, respectively, are drastically impaired in *parp3* morphants. Moreover, there is a reduced expression of *neurod*, a transcription factor involved in the differentiation of non-neuronal ectodermal cells into differentiated sensory neurons, in placodes of the trigeminal ganglion, the anterior lateral line and the statoacoustic ganglion. The knock-down of Parp3 results in inner ear loss. Although the downregulation of *neurod* has not been performed yet in zebrafish, the knockdown of its upstream effector, neurogenin1(ngn1), was executed and revealed no external morphological differences in the

developing ear (Andermann et al., 2002). The removal of *neurod* expression seems to be insufficient to impede the whole development of the ear, even though its expression is important for cranial sensory ganglia. The absence of inner ear implies that hair cells are also absent, this could explain the reduced motility of *parp3* morphants because these cells are essential for swimming (Whitfield et al., 2002).While the downregulation of both *dlx3b* and *dlx4b*, in zebrafish, is sufficient to impair the development of otoliths (Esterberg and Fritz, 2009), the loss of function of both Sox9a and Sox9b result in complete ear loss (Yan et al., 2004). Perhaps *sox9b* expression is also reduced in *parp3* morphants since Sox9a and Sox9b act in a synergistic manner to regulate neural crest cells (Yan et al., 2005) or the combined effect of the reduced expression of *dlx3b/dlx4b* with *sox9a* is sufficient to lead to this phenotype. The loss of pectoral fins also indicates that *sox9b* expression is potentially impaired since *sox9* orthologues have synergistic effect. However, the knockdown of these two orthologues leads to the loss of chondral bones but not the dermal bones (cleithrum) of the pectoral fins (Yan et al., 2005). This indicates that other genetic aberrations resulting from the knock-down of Parp3 are responsible for the loss of the pectoral fins in *parp3* morphants. Noteworthy, the loss of pectoral fins can potentially perturb the swimming of the morphants.

4.3 The putative mechanisms of action of PARP3

The reduced expression of *sox9a*, *dlx3b*/*dlx4b* and *neurod* in Parp3 zebrafish morphants indicates that PARP3 is required for maintaining normal expression levels of these key developmental genes. This observation was unexpected, in view of the association of PARP3 with PRC2 and the significant overlap between PARP3-bound and PcG-bound gene targets (Fig. 1.5B) that rather

suggested a repressor function for Parp3. Furthermore, the regulation of *Sox9* by PRC2 in mouse ES cells has been recently demonstrated (Peng et al., 2009). The relationship existing between PARP3 and PRC2 components may be context dependent, for example occurring in cells at a specific stage of lineage commitment, or in specific cell types. Nonetheless, given that only part of the nuclear PARP3 pool is associated with Polycomb bodies (Fig.1.3), our data could indicate that the transcriptional activation of s*ox9a, dlx3b, dlx4b* and *neurod* by Parp3 is independent of its association with PRC2. Congruent with this idea, poly(ADP-ribosyl)ation of histones contributes significantly to the decondensation of chromatin (Ji and Tulin, 2010). Although mostly characterized in the context of PARP1-dependent poly(ADPribosyl)ation, histone H1 modification in vitro by PARP3 has been reported recently (Loseva et al., 2010; Rulten et al., 2011) supporting the notion that PARP3 could also participate in chromatin remodelling at specific loci. Alternatively, it is conceivable that Parp3 could modulate the repression exerted by PRC2 at specific time points during development. In mouse ES cells, Sox9 is in a bivalent domain, meaning that it is located in a region enriched for both the transcription repressive mark H3K27me3 and activating mark H3K4me3 (Peng et al., 2009). The limited understanding of bivalent genomic regions suggests that this epigenetic context allows maintaining the silencing of developmental regulators while at the same time keeping them ready for transcriptional activation at a later developmental stage (Mikkelsen et al., 2007; Schwartz et al., 2009). The regulated transition from fully silenced to fully expressed genes has been proposed to be mediated by proteins of the Trithorax complex and of PRC1 both in mouse ES cells and neural progenitor cells (Shen et al., 2008; Mikkelsen et al., 2007; Schwartz et al., 2009). It is conceivable that PARP3 participates in the transition between the bivalent K4me3+K27me3 state to the activated K4me3 state.

4.4 *Parp3* morphants display abnormalities in structures originating from the NC

In addition to the reduction of neural crest specifiers, zebrafish *parp3* morphants exhibit a reduced expression of the neural crest marker crestin. Together, it suggests that the accurate development of the neural crest is dependent on the expression of Parp3. This affirmation is reinforced by the fact that neural crest derivative structures are perturbed in these morphants. First, although we do not possess direct evidence about the loss of melanocytes, the reduced pigmentation in *parp3* morphants suggests that melanocyte formation is dependent on Parp3 expression. Moreover, the reduction is MO concentration-dependent. Second, the mesenchymal cells that are migrating along the path of the actinotrichias in wild type zebrafish larvae are disorganized in *parp3* morphants. Neural crest cells are thought to contribute to the mesenchyme tissue in the fins of zebrafish (Smith and al., 1994) albeit it is uncertain whether it's this contribution that will later form the bony lepidotrichia (Suzuki et al., 2003), the migrating mesenchymal cells are severely perturbed in *parp3* morphants. The last neural crest-derived structure that remains to be examined in *parp3* morphants are craniofacial elements. Despite a lack of data, we can speculate that they are severely perturbed in *parp3* morphants since the synergistic action of Sox9 co-orthologs precludes the formation of cranial cartilages.

4.5 The role of zebrafish Parp3 appears distinct from that of Parp1

Among the PARP family, PARP3 is mostly related to PARP1and PARP2. A previous study has shown that *Parp1*$^{-/-}$ and *Parp2*$^{-/-}$ mice develop normally but display a hypersensitivity to DNA damaging agents (Ménissier de Murcia et al., 2003). However, the simultaneous knock-out of both genes in mice results in early embryonic lethality, revealing a functional redundancy

between these two PARPs during DNA damage repair and during mouse development (Ménissier de Murcia et al., 2003). The lethality observed in *Parp1*$^{-/-}$*/Parp2*$^{-/-}$ mice further indicated that PARP3 cannot compensate for the absence of PARP1 and PARP2 during mouse development. The work presented in thesis now reveals that Parp3 is essential for zebrafish development, implying that Parp1 and Parp2 cannot compensate for the biological functions of Parp3 during development. To better support the notion that Parp3 functions are distinct from those of Parp1 and Parp2 during zebrafish development, I produced and characterized *parp1* and *parp2* morphants as well as *parp1/parp2* morphants. The results suggest a functional difference between Parp3 and Parp1. While *parp2* morphants develop normally, median fin fold development is perturbed in most *parp1* morphants and one out of three embryos display a curved tail pointing in random directions and smaller size similar to *parp3* morphants. The *parp1* morphants do not exhibit most of the phenotypes observed in *parp3* morphants, that is: pigmentation, inner ear and pectoral fin fold develop normally and motility of *parp1* morphants is normal. Additionally, like *parp2* morphants, the life span of these Parp1-deficient embryos is not impaired as opposed to *parp3* morphants. Unlike Parp1$^{-/-}$/Parp2$^{-/-}$ mice, *parp1/parp2* morphants survive and embryo development is similar to wt. However, the knock-down of Parp2 is partial, consequently these data are inconclusive. Although Parp1 and Parp3 are well conserved in zebrafish, Parp2 is less well conserved when compared to the human and mouse orthologues. Parp2 comprises an additional domain, the WWE domain. This domain is known to be involved in protein ubiquitination since it is structurally related to E3 ubiquitin ligases (Aravind, 2001) and could potentially targets proteins for ubiquitination upon ADPr binding (Wang et al., 2012).The WWE domain is found in other human PARPs, namely PARP7 and PARP11 to PARP14 (Amé et al., 2004). This suggests that PARP domain shuffling occurred

throughout vertebrate evolution. As the alignment of the amino sequences of zebrafish Parp3 and human PARP3 demonstrated, Parp3 domains are well conserved in zebrafish validating this animal as a good vertebrate model to study the function of Parp3. Because Parp3 is essential for zebrafish development, it suggests that no other PARPs can compensate for its functions.

4.6 The meaning of induced cell death resulting from Parp3 depletion

Here, the observed phenotypes resulting from Parp3 depletion could be due to the diminished presence of Parp3 itself and/or the diminished poly(ADP-ribosyl)ation activity of Parp3. The Morpholino oligonucleotides strategy employed here blocked the translation of Parp3. It is not clear whether the observed-phenotypes are dependent on the activity of Parp3 because we could not impede specifically the activity of Parp3. I have found that *parp3* knockdown leads to an important increase in apoptosis throughout the embryo. Given the important role of PARPs in the response to DNA damage, a mechanism that requires poly(ADP-ribosyl)ation (Satoh et al., 1992), we can speculate that DNA repair in *parp3* morphants is less efficient thereby leading cells to undergo programmed cell death. A previous study showed that PARP3 interacts with proteins involved in SSBR/BER and non-homologous end joining (NHEJ) pathways (Rouleau et al., 2007) illustrating, for the first time, PARP3 as a player in DNA repair. Two recent studies demonstrated that PARP3 exerts a positive effect on the repair efficiency of DSBs (Rulten et al., 2011; Boehler et al., 2011).To determine whether DNA repair is impaired in *parp3* morphants, supplementary experiments would be needed in the future. For instance, exposure of embryos to γ irradiation with subsequent measure of γH2AX foci numbers could inform us about the ability of *parp3* morphants to repair the DSBs since the number of γH2AX foci within a cell is proportional to the number of DSBs (Löbrich et al., 2010). On the one hand, the decreased signal

of crestin in *parp3* morphants reflects that the number of neural crest cells is reduced, which could result from the transcriptional regulatory role of Parp3 on *sox9a, dlx3b/dlx4b*. Whether cell death is induced after misregulation of *sox* and *dlx* expression or by inefficient DSB repair remains to be defined. On the other hand, perhaps these cells are dying because they need Parp3 to increase their efficiency to repair DNA during early development. Neuronal progenitors are particularly sensitive to DNA damages since DDR-defective disorders show neuronal impaired development and many also display severe microcephaly (O'Driscoll and Jeggo, 2008). The explanation of this phenomenon is likely to be related to the high proliferation and differentiation rate of the neuronal stem cells during neurogenesis combined with a low threshold for apoptosis induction, which render these cells particularly susceptible to DNA damage (O'Driscoll and Jeggo, 2008). To better answer this question, I attempted to perform an experiment that would have localized apoptotic cells with neural crest cells: TdT-mediated dUTP nick-end labeling (TUNEL) combined with ISH, using different fluorescent dye for the dUTP and *crestin* probe. Unfortunately, zebrafish tissue precludes achievement of this experiment.

4.7 The developmental role of Parp3 is consistent with previously identified roles in other PARPs

A number of studies have demonstrated that PARP1, PARP2, PARG and poly(ADP-ribosyl)ation are important determinants for development (Ménissier de Murcia et al., 2003; Tulin et al., 2002; Hannai et al., 2004). *Drosophila* cannot develop beyond the larval stage when their unique Parp or Parg gene is mutated (Tulin et al., 2002; Hannai et al., 2004). Developmental cues induce poly(ADP-ribosyl)ation signalling to promote or repress the transcription and to influence splicing during developmental processes such as: metamorphosis,

gametogenesis and cell differention (Ji and Tulin, 2010). Collectively, it implies that PARPs protein act under physiological conditions to control and support a normal development.

4.8 The function of Parp3 in zebrafish versus in mice

The zebrafish was the first organism in which insights about the physiological functions of Parp3 were gathered (Rouleau et al., 2011). Although zebrafish represents an excellent model in the developmental biology field, it may occur that phenotypes observed in this species are somewhat distinct from those observed in "higher" organisms. Shortly after the publication of the manuscript "A key role for Poly(ADP-Ribose) Polymerase 3 in ectodermal specification and neural crest development", the effect of Parp3 knockout in mice were published (Boehler et al., 2011). Surprisingly, no abnormalities in development were observed. To explain this, it has to be taken into account that compensatory mechanisms exist within PARP family members (Ménissier de Murcia et al., 2003). Likewise, perhaps uncharacterized domains are responsible for PARPs compensation in mice. The N-terminal domain of zebrafish Parp3 is less well conserved (48% similarity) in comparison to the WGR (77% similarity) and catalytic domain (76% similarity). Thus, some important but uncharacterized functions of the N-terminal of Parp3 domain could be responsible for the differences observed between the mouse and the zebrafish. Indeed, the N-terminal domain of the mouse Parp3 is better conserved (74% similarity) suggesting that its putative function is more similar to the human protein than the zebrafish protein is. The possible absence of such particularities within the zebrafish protein could render this organism more susceptible than the mouse. Importantly, we have to remind that the neural plate border specifiers, for which we found a reduced expression in *parp3* morphants, are also bound by PARP3 in a human cell line. Furthermore, other important specifiers of the neural crest

and the preplacodal ectoderm, such as SOX10 and SOX8, are bound by PARP3 in the ChIP-chip experiment.

4.9 Neural crest cell development and neuroblastoma

We hypothesized earlier that PARP3 is an important player in the control of transcription and in the maintenance of genomic integrity of NC cells and that these PARP3-dependent mechanisms are altered in neuroblastoma (NB). Our results are consistent with PARP3 playing a role in the regulation of transcription of neural crest cells since we found that the expression of neural crest specifiers, in zebrafish, are Parp3-dependent. We also proposed that the loss of *crestin* signal was a consequence of apoptosis although the neural crest specificity for apoptosis was not determined empirically. Given the prevalence of the apoptotic signal in *parp3* morphants, several NC cells are inevitably dying albeit other cell types could be undergoing apoptosis in this experiment. It is reasonable to speculate that Parp3 helps to preserve genomic integrity of neural crest cells. Obviously supplementary experiments would be necessary to confirm this part of the hypothesis. In this thesis, we did not investigate the proliferating status of the NC cells in *parp3* morphants. However, developmental defects observed in these morphants could also be attributable to reduced proliferation rates. Indeed, a function of PARP3 during mitosis progression has recently been described (Boehler et al., 2011). As stated in the introduction, *PARP3* is located in chromosomal region 3p21 in human, which is often lost in the poor prognosis 11q genetic subtype of stage 4 NB (Hoebeeck et al., 2007; Nair et al., 2007). Many tumour suppressor genes are likely to be present on chromosomic location 3p21 because other cancers exhibit this deletion, such as lung and breast cancer (Kok et al., 1987; Sediko et al., 1998). The importance of studying the physiological function of PARP3 holds in the quest for the identification of

tumour suppressor genes involved in NB development. A better knowledge of the biological features of NB will help for screening, improved prognosis and selection of therapies and perhaps will allow the development of new therapies. According to our results, PARP3 remains a good candidate for being one, among others, tumour suppressor involved in NB formation. Therefore continued research about its biological function is essential to understand how PARP3 could contribute to NB formation.

Future directions

While the absence of Parp3 precludes normal neural crest development in zebrafish, other studies suggest that PARP3 is involved in the respond to DNA damages, especially in the NHEJ pathway (Rouleau et al., 2007; Rulten et al., 2011; Boehler et al., 2011). These features confer to PARP3 potential roles for the transformation of neural crest cells in neuroblastoma. Further analysis is required to elucidate the detailed mechanisms by which PARP3 is potentially contributing to this type of tumour. It will be useful to continue to examine our vertebrate animal model, the zebrafish, since it is a valuable *in vivo* model for studying the function of Parp3 during NC development. First, the focus should be on determining the contribution of Parp3 to the genomic integrity of NC cells. For instance, we can assess the ability of *parp3* morphants to repair DSBs, in this cell type. We could also survey cell proliferations rates of NC in these morphants to determine whether Parp3 also exerts such effects in these cells. It is possible to monitor cell proliferation rates by staining zebrafish with human phosphohistone-H3 antibodies since it is well conserved between species (Derup et al., 2009). It will be crucial to address whether the catalytic activity of Parp3 is essential to produce the developmental abnormalities observed in zebrafish by conducting rescue experiments with zebrafish mRNA of *parp3* mutated

in the catalytic site and in the MO-targeting sites. The association of PARP3 with PRC2 complex led to the hypothesis that PARP3 counteracts with the methyltransferase activity of EZH2 by interacting with components of the PRC2 complex thereby inducing the expression of PRC2 targets. A ChiP-qPCR analysis of the H3k27me3 genomic occupancy could be performed at and under 24hpf in *parp3* morphants and wild type. In parallel to explorations *in vivo*, NB cell lines could be used to understand the contribution of PARP3 to neuroblastoma proliferation. Using a set of NB cell lines with defined genetic backgrounds, such as some with the 3p deletion employed as test and some without the 3p deletion employed as control, it is conceivable to study the effects of PARP3 on cell death, cell proliferation and cell cycle progression by transfecting the NB cell lines with *PARP3* gene. Moreover, many experiments performed in NB could be complemented with expression of *PARP3* mutated in catalytic site. The above questions require more attention in the future and can be answered with different experiments involving either our vertebrate animal model or the NB cell lines.

Conclusion

The data presented in this thesis provided the first insights into the biological functions of the PARP family member PARP3. Indeed, the zebrafish is the first animal model for which the loss-of-function experiment of Parp3 triggers developmental abnormalities. We identify PARP3 as an important transcriptional regulator acting early in the development of sensory placodes and in the specification of neural crest cells of zebrafish embryos. Moreover, cell survival is Parp3-dependent during early stages of their development. The developmental functions of PARP3 are distinct from those of PARP1 and PARP2. My analysis suggests that the function of zebrafish Parp1 is indeed different from that of Parp3. However, it is inconclusive for Parp2. Taken as a

whole, our findings suggest that PARP3 is an early key component in the regulation of the neural plate border formation in vertebrates.

References

Akimenko MA, Ekker M, Wegner J, Lin W, Westerfield M (1994) Combinatorial expression of three zebrafish genes related to distal-less: part of a homeobox gene code for the head. *J Neurosci* 14: 3475-3486

Althaus FR and Richter C (1987) ADP-ribosylation of proteins: enzymology and biological significance. *Mol biol, biochem, and biophysics* 37: 1-237

Amé J-C, Rolli V, Schreiber V, Niedergang C, Apioui F, Decker P, Muller S, Höger T, Ménissier-de Murcia J, de Murcia G (1999) PARP-2, A Novel Mammalian DNA Damage-dependent Poly(ADP-ribose) Polymerase. *J Biol Chem* 274: 17860–17868

Amé J-C, Spenlehauer C, De Murcia G (2004) The PARP superfamily. *BioEssays* 26: (8) 882-893

Andermann P, Ungos J, Raible DW (2002) Neurogenin1 defines zebrafish cranial sensory ganglia precursors. *Dev Biol* 251: 45-58

Aravind L (2001) The WWE domain: a common interaction module in protein ubiquitination and ADP ribosylation. *Trends Biochem Sci* 26: (5) 273-275

Augustin A, Spenlehauer C, Dumond H, Menissier-De Murcia J, Piel M, Schmit A-C, Apiou F, Vonesch J-L, Kock M, Bornens M, De Murcia G (2003) PARP-3 localizes preferentially to the daughter centriole and interferes with the G1/S cell cycle progression. *J Cell Sci* 116:1551-156

Bai P, Houten SM, Huber A, Schreiber V, Watanabe M, Kiss B, De Murcia G, Auwerx J, Ménissier-de Murcia J (2007) Peroxisome Proliferator-activated Receptor (PPAR)-2 controls adipocyte differentiation and adipose tissue function through the regulation of the activity of the Retinoid X Receptor/PPAR heterodimer. *J Biol Chem* 282: (52) 37738-37746

Boehler C, Gauthier LR, Mortusewicz O, Biard DS, Saliou J-M , Bresson A, Sanglier-Cianferani S, Smith S, Schreiber V, Boussin F, and Dantzer F (2011) Poly(ADP-ribose) polymerase 3 (PARP3), a newcomer in cellular response to DNA damage and mitotic progression. *PNAS* 108: (7) 2783-2788

Bracken AP, Dietrich N, Pasini D, Hansen KH, Helin K (2006) Genome-wide mapping of Polycomb target genes unravels their roles in cell fate transitions. *Genes Dev* 20: 1123-1136.

Brodeur GM (2003) Neuroblastoma: biological insights into a clinical enigma. *Nat Rev Cancer* 3: 203-216

Burzio LO, Riquelme PT and Koide SS (1979) ADP ribolysation of rat liver nucleosomal core histones. *J Biol Chem* 254: 3029-3037

Concha II, Figueroa J, Concha MI, Ueda K, Burzio LO (1989) Intra-cellular distribution of poly(ADP-ribose) synthetase in rat spermatogenic cells. *Exp Cell Res* 180:353–366

Chambon P, Weil JD, Doly J, Strosser MT, Mandel P (1966) On the formation of a novel adenylic compound by enzymatic extracts of liver nuclei. *Biochem Biophys Res Commun* 25: 638-643

Cherney BW, Mcbride OW, Chen D, Alkhatib H, Bhatia K, Hensley P and Samulson ME (1987) cDNA sequence, protein structure, and chromosomal location of the human gene for poly(ADP-ribose) polymerase. *Proc Natl Aca. Sci USA* 84: 8370-8374

Collier RJ and Pappenheimer AM (1964) Studies on the mode of action of diphtheria toxin-II: effect of toxin on amino acid incorporation in cell-free systems. 1964. *J Exp Med* 120**:** 1019-1039

D'Amours D, Desnoyers S, D'Silva I, Poirier GG (1999) Poly(ADP-ribosyl)ation reactions in the regulation of nuclear functions. *Biochem J* 342: 249-268

Dantzer F, Mark M, Quenet D, Scherthan H, Huber A, Liebe B, Monaco L, Chicheportiche A, Sassone-Corsi P, De Murcia G, Ménissier-de Murcia J (2006) Poly(ADP-ribose) polymerase-2 contributes to the fidelity of male meiosis I and spermiogenesis. *PNAS* 103: (40) 14854-14859

Desnoyers S, Shah G, Brochu G, Hoflack J. C, Verreault A, Poirier GG (1995) Biochemical properties and function of poly(ADPribose) glycohydrolase. *Biochimie* 77: 433-438

Drerup CM, Wiora, HM, Topczewski J, Morris JA (2009) Disc1 regulates foxd3 and sox10 expression, affecting neural crest migration and differentiation. *Development* 136: 2623-32

Durán I, Marí-Beffa M, Santamaría JA, Becerra J, Santos-Ruiz L (2011) Actinotrichia collagens and their role in fin formation. *Dev Biol* 354: 160-172

Elsalini OA, von Gartzen J, Cramer M, Rohr KB (2003) Zebrafish hhex, nk2.1a, and pax2.1 regulate thyroid growth and differentiation downstream of Nodal dependent transcription factors. *Dev Biol* 263: 67-80

Esterberg R and Fritz A (2009) dlx3b/4b are required for the formation of the preplacodal region and otic placode through local modulation of BMP activity. *Dev Biol* 325: 189-199

Francis NJ and Kingston RE (2001) Mechanisms of transcriptional memory. *Nat Rev Mol Cell Biol* 2: (6) 409-421

Haince J-F, Rouleau M, Hendzel MJ, Masson J-Y, Poirier GG (2005) Targeting poly(ADP-ribosyl)ation: a promising approach in cancer therapy. *Trends in Molecular Medicine* 11: (10) 456-463

Haldin CE and LaBonne C (2010) SoxE factors as multifunctional neural crest regulatory factors. *Int J Biochem Cell Biol* 42: 441-444

Hall BK (2000) The neural crest as a fourth germ layer and vertebrates as quadroblastic not triploblastic. *Evolution and Development* 3: (1) 3-5

Hanai S, Kanai M, Ohashi S, Okamoto K, Yamada M, et al. (2004) Loss of poly(ADP-ribose) glycohydrolase causes progressive neurodegeneration in Drosophila melanogaster. *Proc Natl Acad Sci USA* 101: 82-86

Hassa PO, Haenni SS, Elser M, Hottiger MO (2006) Nuclear ADP-ribolylation reactions in mammalian cells: Where are we today and where are we going? *Microbiol and Mol Biol Rev* 70: (3) 789-829

Hoebeeck J, Michels E, Menten B, Van Roy N, Eggert A, Schramm A, De Preter K, Yigit N, De Smet E, De Paepe A, Laureys G, Vandesompele J, Speleman F (2007) High resolution tiling-path BAC array deletion mapping suggests commonly involved 3p21-p22 tumor suppressor genes in neuroblastoma and more frequent tumors. *Int J Cancer* 120: 533-8.

Hottiger MO, Hassa PO, Lüscher B, Schüler H, Koch-Nolte F (2010) Toward a unified nomenclature for mammalian ADP-ribosyltransferase. *Trends biochem Sci* 35: (4) 208-219

Ji Y, Tulin AV (2010) The roles of PARP1 in gene control and cell differentiation. *Curr Opin Genet Dev* 20: 512-518

Jiang M, Stanke J, Lahti JM (2011) The connections between neural crest development and neuroblastoma. *Curr Top Dev Biol* 94: 77-127

Johansson M (1999) A human poly(ADP-ribose)polymerase gene family (ADPRTL): cDNAcloning of two novel poly(ADP-ribose) polymerase homologues. *Genomics* 57: 442-445

Kameshita I, Matsuda Z, Taniguchi T, Shizuta Y (1984) Separation and identification of three proteolytic fragments as the substrate-binding domain, the DNA-binding domain, and the automodification domain *J Biol Chem* 259: (8) 4770-4776

Kaminker PG, Kim S-H,Taylor RD, Zebarjadian Y, Funk WD, Morin GB, Yaswen P, Campisi J (2001) TANK2, a new TRF1-associated Poly(ADP-ribose) Polymerase, causes rapid induction of cell death upon overexpression. *J Biol Chem* 276: (38) 35891-35899

Kickhoefer VA, Sivaa AC, Kedershab NL, Inmana EM, Rulanda C, Streulic M, Rome LH (1999) The 193-Kd Vault Protein, Vparp, is a novel Poly(Adp-Ribose) Polymerase. *J Cell Biol* 146: (5) 917-928

Kimmel CB, Ballard WW, Kimmel SR, Ullmann B, Schilling TF (1995) Stages of embryonic development of the zebrafish. *Dev dyn* 203: (3) 253-310

Kleine H, Poreba E, Lesniewicz K, Hassa PO, Hottiger MO, Litchfield D, Shilton BH, Lüscher B (2008) Substrate-assisted catalysis by PARP10 limits its activity to mono-ADP-ribosylation. *Mol Cell* 32: 57-69

Kok k, Osinga J, Carritt B, Davis MB, Van Der Hout AH, Van Der Veen AY, Landsvater RM et al. (1987) Deletion of a DNA sequence at the chromosomal region 3p21 in all major types of lung cancer. *Nature* 330: 578-581

Lawson ND and Weinstein BM (2002) In vivo imaging of embryonic vascular development using transgenic zebrafish. *Dev Biol* 248: 307-318

Lee TI, Jenner R.G, Boyer LA, Guenther MG, Levine SS, et al. (2006) Control of developmental regulators by Polycomb in human embryonic stem cells. *Cell* 125: 301-313

Levine SS, King IFG, Kingston RE (2004) Division of labor in Polycomb group repression. *Trends in Biochem Sci* 29: (9) 478-485

Löbrich M, Shibata A, Beucher A, Fisher A, Ensminger M, Goodarzi AA, Barton O, Jeggo PA γH2AX foci analysis for monitoring DNA double-strand break repair. Strengths, limitations and optimization. *Cell cycle* 9: (4) 662-669

Loseva O, Jemth AS, Bryant HE, Schuler H, Lehtio L, et al. (2010) PARP-3 is a mono-ADP-ribosylase that activates PARP-1 in the absence of DNA. *J Biol Chem* 285: 8054-8060.

Luo R, An M, Arduini BL, Henion PD (2001) Specific pan-neural crest expression of zebrafish Crestin throughout embryonic development. *Dev Dyn* 220: 169-174

Maris, JM, Hogarty MD, Bagatell R, Cohn SL (2007) Neuroblastoma. *The Lancet* 369: (9579) 2106-20

Meder VS, Boeglin M, De Murcia G, Schreiber V (2005) PARP-1 and PARP-2 interact with nucleophosmin/B23 and accumulate in transcriptionally active nucleoli. *J Cell Sci* 118: 211-222.

Mikkelsen TS, Ku M, Jaffe DB, Issac B, Lieberman E, et al. (2007) Genome-wide maps of chromatin state in pluripotent and lineage-committed cells. *Nature* 448: 553-560

Menegazzi M, Grassi-Zucconi G, Carcerero De Prati A, Ogura T, Poltronieri P, Nyunoya H, Shiratori-Nyunoya Y. Miwa M, Suzuki H (1991) Differential expression of poly(ADP-ribose) polymerase and DNA polymerase beta in rat tissues. *Exp Cell Res* 197:66-74

Ménissier de Murcia J, Niedergang, Trucco C, Ricoul M, Dutrillaux B, Mark M, Olivier FJ, Masson M, Dierich A, Lemeur M, Walztinger C, Cnambon P, De Murcia J (1997) Requirement of poly(ADP-ribose) polymerase in recovery from DNA damage in mice and in cells. *Proc Natl Acad Sci USA* 94: 7303-7307

Ménissier de Murcia J, Ricoul M, Tartier L, Niedergang C, Huber A, Dantzer F, Schreiber V, Ame JC, Dierich A, LeMeur M et al. (2003) Functional interaction between PARP-1 and PARP-2 in chromosome stability and embryonic development in mouse. *EMBO J* 22: 2255-2263

Messner S, Matthias Altmeyer M, Zhao H, Pozivil A, Roschitzki B, Gehrig P, Rutishauser D, Huang D, Caflisch A, Hottiger MO (2010) PARP1 ADP-ribosylates lysine residues of the core histone tails. *Nucl Acids Res* 38 (19): 6350-6362

Miwa M and Sigumira T (1984) Quantification of in vivo levels of poly(AdP-ribose): Tritium labelling method and radioimmunoassay. *Meth Ezym* 106: 441-450

Nair PN, McArdle L, Cornell J, Cohn SL, Stallings RL (2007) High-resolution analysis of 3p deletion in neuroblastoma and differential methylation of the SEMA3B tumor suppressor gene. *Cancer Genet Cytogenet* 174: 100-10

Nasevicius A and Ekker SC (2000) Effective targeted gene “knockdown” in zebrafish. *Nature Genetics* 26: 216-220

Nishikimi M, Ogasawara K, Kameshita I, Taniguchi T, Shizuta Y (1982*)* Poly(ADP-ribose) Synthetase. The DNA binding domain and the automodification domain. *J Biol Chem* 257: (11) 6102-6105

O'Driscoll M, Jeggo PA (2008) The role of the DNA damage response pathways in brain development end microcephaly: Insight from human desorders. *DNA repair* 7: 1039-1050

Oka J, Ueda K, Hayaishi O, Komura H, Nakanishi K (1984) ADP-ribosyl protein lyase. Purification, properties, and identification of the product. *J Biol Chem* 259: 986-995

Oliver AW, Amé J-C, Roe SM, Good V De Murcia G,Pearl LH (2004) Crystal structure of the catalytic fragment of murine poly(ADP-ribose) polymerase-2. *Nucl Acids Res* (2004) 32 (2): 456-464

Otto H, Reche PA, Bazan F, Dittmar K, Haag F, Koch-Nolte F. (2005) In silico characterization of the family of PARP-like poly(ADP ribosyl) transferases (pARTs). *BMC Genomics* 6:139

Peng JC, Valouev A, Swigut T, Zhang J, Zhao Y, Sidow A, Wysocka J (2009) Jarid2/Jumonji coordinates control of PRC2 enzymatic activity and target gene occupancy in pluripotent cells. *Cell* 139: 1290-1302.

Poirier GG, De Murcia G, Jongstra-Bilen J, Niedergang C, Mandel P. (1982) Poly(ADP-ribosyl)ation of polynucleosomes causes relaxation of chromatin structure. *Proc Natl Acad Sci USA* 79: 3423-3427

Rau M, Fischer S, Neumann CJ (2006) Zebrafish Trap230/Med12 is required as a coactivator for Sox9-dependent neural crest, cartilage and ear development. *Dev Biol* 296: (1)83-93

Riquelme PT, Burzio LO, Koide SS (1979) ADP ribosylation of rat liver lysin-rich histone in vitro. *J Biol Chem* 254: 3018-3028

Rouleau M, Aubin RA, Poirier GG (2004) Poly(ADP-ribosyl)ated chromatin domains :access granted. *J Cell Science* 117: 815-825

Rouleau M, El-Alfy M, Lévesque M-H et Poirier GG (2009) Assessment of PARP-3 distribution in tissues of cynomolgous monkeys. *J Histochem Cytochem* 57:675-685

Rouleau M, McDonald D, Gagné P, Ouellet M-E, Droit A, Hunter J-M, Dutertre S, Prigent C, Hendzel M-J et Poirier GG (2007) PARP-3 associates with polycomb group bodies and with components of the DNA damage repair machinery. *J Cell Biochem* 100: 385-401

Rouleau M, Saxena V , Rodrigue A , Paquet ER, Gagnon A, Hendzel MJ, Masson J-Y, Ekker M, Poirier GG (2011) A key role for Poly(ADP) Polymerase 3 in ectodermal specification and neural crest development. *PLoS one* 6: e15834

Robu ME, Larson JD, Nasevicius A, Beiraghi S, Brenner C, Farber SA, Ekker SC (2007) p53 activation by knockdown technologies. *PLoS Genetics* 3: (5) 787-801

Ruf A, Rolli V, de Murcia G, Schulz GE (1998) The mechanism of the elongation and branching reaction of poly(ADP-ribose)polymerase as derived from crystal structures and mutagenesis. *J Mol Biol* 278:57-65

Rohr KB, Barth KA, Varga ZM, Wilson SW (2001) The nodal pathway acts upstream of hedgehog signaling to specify ventral telencephalic identity. *Neuron* 29: 341-351

Rulten SL, Fisher AEO, Robert I, Zuma MC, Rouleau M, Ju L ,Poirier GG, Reina-San-Martin B, Caldecott KW (2011) PARP-3 and APLF function together to accelerate nonhomologous end-joining. *Mol Cell* 41:33-45

Santamaría J and Becerra J (1991) Tail fin regeneration in teleosts: cell-extracellular matrix interaction in blastemal differentiation. *J Anat* 176: 9-21

Santamaría JA, Marí-Beffa M, Becerra J (1992) Interactions of the lepidotrichial matrix components during tail fin regeneration in teleosts. *Differentiation* 49: 143-150

Satoh MS and Lindahl T (1992) Role of poly(ADP-ribose) formation in DNA repair. *Nature (London)* 356: 356-358.

Sauka-Spengler T and Bronner-Fraser M (2008) A gene regulatory network orchestrates neural crest formation. *Nat Rev Mol Cell Biol* 9: 557-568.

Schreiber V, Amé J-C, Dollé P, Schultz I, Rinaldi B, Fraulob V, Ménissier-de Murcia J, De Murcia G (2002) Poly(ADP-ribose) polymerase-2 (PARP-2) Is Required for Efficient Base Excision DNA Repair in Association with PARP-1 and XRCC1. *J Biol Chem* 277: 23028-23036

Schuettengruber B, Chourrout D, Vervoort M, Leblanc B, Cavalli G (2007) Genome regulation by polycomb and trithorax Proteins. *Cell* 128: 735-745

Schwartz YB, Kahn TG, Stenberg P, Ohno K, Bourgon R, et al. (2009) Alternative epigenetic chromatin states of polycomb target genes. *PLoS Genet* 6:e1000805.

Sekido Y, Ahmadian M, Wistuba I, Latif F, Bader S, Wei M-H, Duh F-M, Gazdar AF, Lerman MI, Minna JD (1998) Cloning of a breast cancer homozygous deletion junction narrows the region of search for a 3p21.3 tumor suppressor gene. *Oncogene* 16: 3151-3157

Shah GM, Poirier D, Duchaine C, Brochu G, Desnoyers S, Jean L, Verreault A, Hoflack J-C, Kirkland JB, Poirier GG (1995) Methods for biochemical study of poly(ADP-ribose) metabolism in vitro and in vivo. *Anal biochem* 227: (1) 1-13

Shen X, Liu Y, Hsu YJ, Fujiwara Y, Kim J, et al. (2008) EZH1 mediates methylation on histone H3 lysine 27 and complements EZH2 in maintaining stem cell identity and executing pluripotency. *Mol Cell* 32: 491-502

Shieh WM, Ame JC, Wilson MV, Wang ZQ, Koh DW, Jacobson MK, Jacobson EL (1998) Poly(ADP-ribose) polymerase null mouse cells synthesize ADP-ribose polymers. *J Biol Chem* 273: 30069-30072

Shu X, Zeng Z, Gautier P, Lennon A, Gakovic M, Patton EE, Wright AF (2010) Zebrafish Rpgr is required for normal retinal development and plays a role in dynein-based retrograde transport processes. *Human Molecular Genetics* 19: (4) 657-670

Smith M, Hickman A, Amanze D, Lumsden A, Thorogood P (1994) Trunk neural crest origin of caudal fin mesenchyme in the zebrafish Brachydanio rerio. *Proceedings of the royal society B: Biol Sci* 256: (1346) 137-145

Smith S, Giriat I, Schmitt A, De Lange T (1998) Tankyrase, a poly(ADP-Ribose) polymerase at Human Telomeres. *Sciences* 282: (5393) 1484-1484

Solomon KS and Fritz A (2002) Concerted action of two dlx paralogs in sensory placode formation. *Development* 129: 3127-3136

Suzuki T, Haga Y, Takeuchi T, Uji S, Hashimoto H, Kurokawa T (2003) Differentiation of chondrocytes and scleroblasts during dorsal fin skeletogenesis in flounder larvae. *Develop. Growth Differ* 45: 435-448

Thisse B, Thisse C (2004) Fast Release Clones: A High Throughput Expression Analysis. ZFIN Direct Data Submission (http://zfin.org).

Thisse C, Thisse B (2008) High-resolution in situ hybridization to whole-mount zebrafish embryos. *Nat Protoc* 3: 59-69

Tucker and Lardelli (2007) A rapid apoptosis assay measuring relative acridine orange fluorescence in zebrafish embryos. *Zebrafish* 4: (2) 113-116

Tulin A, Stewart D, Spradling AC (2002) The Drosophila heterochromatic gene encoding poly(ADP-ribose) polymerase (PARP) is required to modulate chromatin structure during development. *Genes Dev* 16: 2108-2119

Walters KB, Dodd ME, Mathias JR, Gallagher AJ, Bennin DA, Rhodes J, Kanki JP, Look AT, Grinblat Y, Huttenlocher A (2009) Muscle degeneration and leukocyte infiltration caused by mutation of zebrafish fad24. *Dev Dyn* 238: (1) 86-99

Wang Z, Gregory AM, Cheng Z, Zhang Y, Hinds TR, Fan E, Cong F, Xu W (2012) Recognition of the iso-ADP-ribose moiety in poly(ADP-ribose) by WWE domains suggests a general mechanism for poly(ADP-ribosyl)ation-dependent ubiquitination. *Genes Dev* 26: (1) 1-7

Westerfield M (2000) The zebrafish book. 4th ed. Eugene: University of Oregon Press.

Whitfield TT, Riley BB, Chiang M-Y, Philips B (2002) Development of the zebrafish inner ear. *Dev Dyn* 223: 427-458

Wilkie AO and Morriss-Kay GM (2001) Genetics of craniofacial development and malformation. *Nat Rev Genet* 2: (6) 458-468

Wood A and Thorogood P (1984) An analysis of in vitro cell migration during teleost fin morphogenesis. *J Cell Sci 66*: 205-222

Yamanaka H, Penning CA, Willis EH, Wasson B, Carson DA (1988) Characterization of Human poly(ADP-ribose) polymerase with Autoantibodies. *J Biol Chem* 263: (8) 3879-3883

Yan YL, Willoughby J, Liu D, Crump JG, Wilson C, Miller CT, Singer A, Kimmel C, Westerfield M, Postlehwait JH (2005) A pair of Sox: distinct and overlapping functions of zebrafish sox9 co-orthologs in craniofacial and pectoral fin development. *Development* 132: 1069-1083

Yélamos J, Farres J, Ampurdanes C, Martin-Caballero J (2011) PARP1 and PARP2: New players in tumour development. *Am J Cancer Res* 1: (3) 328-346

Yélamos J, Monreal Y, Saenz L, Aguado E, Schreiber V, Mota R, Fuente T, Minguela A, Parrilla P, De Murcia G, Almarza E, Aparicio P, Ménissier-de Murcia J (2006) PARP-2 deficiency affects the survival of CD4+CD8+ double-positive thymocytes. *EMBO J* 25: 4350-4360

Yélamos J, Schreiber V, Dantzer F (2008) Toward specific functions of poly(ADP-ribose) polymerase-2. *Trends in mol med* 14: 169-178

Zhang J, Wagh P, Guay D, Sanchez-Pulido L, Padhi BK, Korzh V, Andrade-Navarro MA, Akimenko M-A (2010) Loss of fish actinotrichia proteins and the fin-to-limb transition. *Nature* 466: (7303) 234-237